



Australian Government
Geoscience Australia

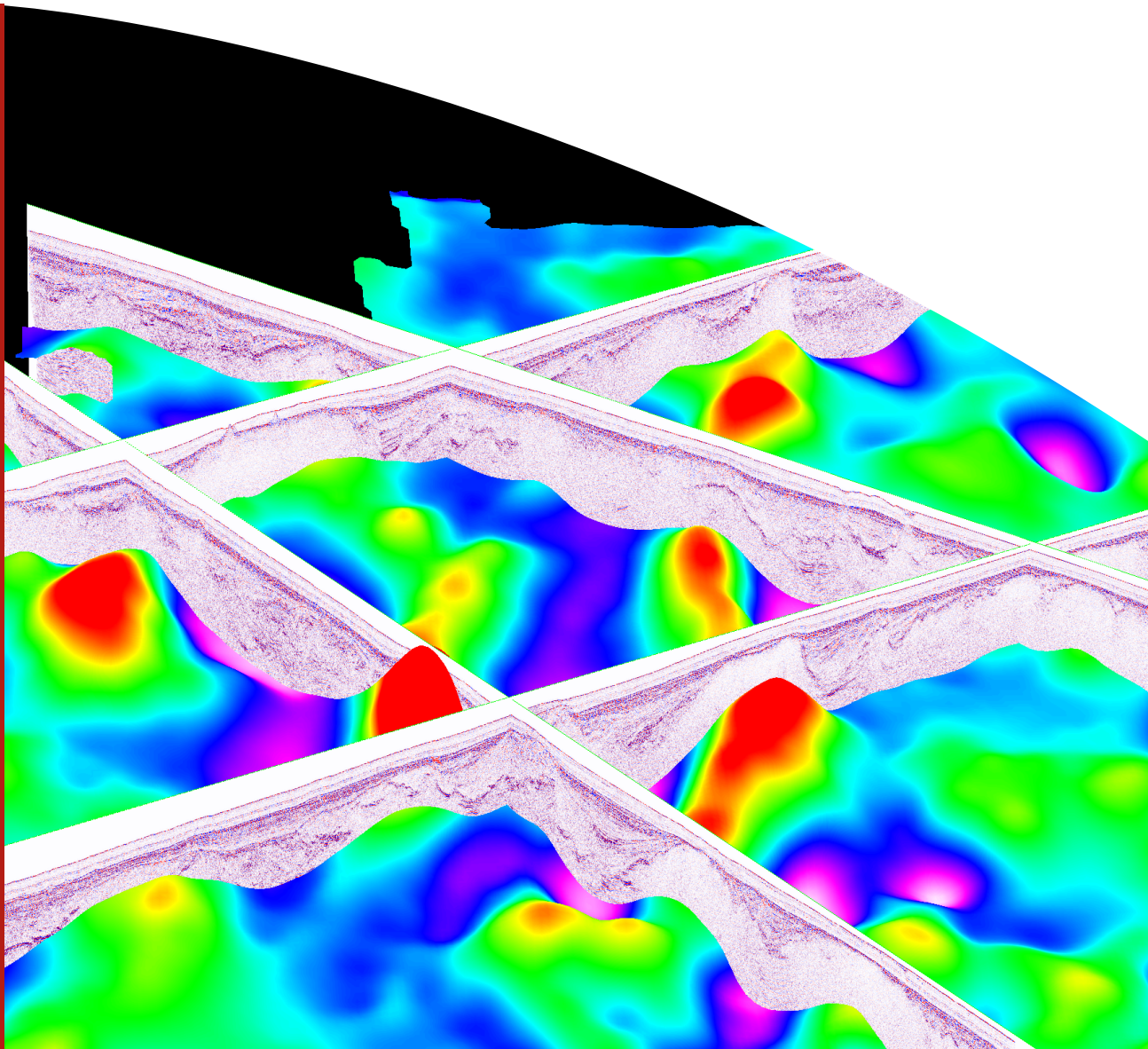
Potential-field data covering the Capel and Faust Basins, Australia's Remote Offshore Eastern Frontier

Ron Hackney

Record

2010/34

**GeoCat #
70711**



Potential-field data covering the Capel and Faust Basins, Australia's Remote Offshore Eastern Frontier

GEOSCIENCE AUSTRALIA
RECORD 2010/34

by

Ron Hackney¹



Australian Government
Geoscience Australia

1. Petroleum and Marine Division, Geoscience Australia, GPO Box 378, Canberra ACT 2601

Department of Resources, Energy and Tourism

Minister for Resources and Energy: The Hon. Martin Ferguson, AM MP

Secretary: Mr Drew Clark

Geoscience Australia

Chief Executive Officer: Dr Chris Pigram



© Commonwealth of Australia, 2010

This work is copyright. Apart from any fair dealings for the purpose of study, research, criticism, or review, as permitted under the *Copyright Act 1968*, no part may be reproduced by any process without written permission. Copyright is the responsibility of the Chief Executive Officer, Geoscience Australia. Requests and enquiries should be directed to the **Chief Executive Officer, Geoscience Australia, GPO Box 378 Canberra ACT 2601**.

Geoscience Australia has tried to make the information in this product as accurate as possible. However, it does not guarantee that the information is totally accurate or complete. Therefore, you should not solely rely on this information when making a commercial decision.

ISSN 1448-2177

ISBN 978-1-921781-36-0 (web)

ISBN 978-1-921781-37-7 (CD/DVD)

GeoCat # 70711

GeoMet # 14435

ANZLIC ID # ANZCW0703014435

Bibliographic reference: Hackney, R., 2010. Potential-field Data Covering the Capel and Faust Basins, Australia's Remote Offshore Eastern Frontier. Geoscience Australia Record 2010/34, 40pp.

Contents

| | |
|---|------------|
| Contents | iii |
| Executive Summary | iv |
| 1 Introduction | 1 |
| 2 Existing data | 3 |
| 2.1 Satellite-derived gravity data | 3 |
| 2.1.1 Datasets from Scripps Institution of Oceanography | 3 |
| 2.1.2 Datasets from the Danish National Space Centre | 6 |
| 2.2 Global compilations of magnetic data | 6 |
| 2.3 Marine data | 9 |
| 2.3.1 Levelled marine data | 9 |
| 2.3.2 Post-2001 marine surveys | 12 |
| 3 Bathymetry data | 13 |
| 4 Capel/Faust potential-field data | 15 |
| 4.1 Survey GA-302 | 15 |
| 4.1.1 Acquisition | 15 |
| 4.1.2 Processing | 15 |
| 4.2 Survey GA-2436 | 16 |
| 4.2.1 Acquisition | 16 |
| 4.2.2 Processing | 16 |
| 4.3 Preliminary combination of data | 17 |
| 5 Levelled marine potential-field data | 19 |
| 5.1 Description of the levelling process | 19 |
| 5.1.1 Data import | 19 |
| 5.1.2 Line splitting | 20 |
| 5.1.3 Line filtering | 21 |
| 5.1.4 Line-levelling method | 21 |
| 5.2 Gravity data levelling | 23 |
| 5.2.1 Line editing | 23 |
| 5.2.2 Levelling | 23 |
| 5.3 Magnetic data levelling | 24 |
| 5.3.1 Line editing | 24 |
| 5.3.2 Levelling | 24 |
| 6 Further data processing | 28 |
| 6.1 Gravity Data | 28 |
| 6.1.1 Bouguer anomaly | 28 |
| 6.1.2 Band-pass filtering | 28 |
| 6.2 Magnetic Data | 31 |
| 6.2.1 Reduction to pole | 31 |
| 7 Summary | 34 |
| Acknowledgements | 34 |
| 8 Appendix: data description | 35 |
| 8.1 File-naming convention | 35 |
| 8.2 Data files | 35 |
| 8.2.1 Data for surveys GA-302 and GA-2436 | 35 |
| 8.2.2 Levelled gravity and magnetic data | 35 |
| 8.2.3 Shape files | 36 |
| 8.3 Gridded data | 37 |
| 8.3.1 Grids of levelled data | 37 |
| 8.3.2 Grids of externally-sourced regional data | 37 |
| References | 38 |

Executive Summary

As part of two major Australian Government initiatives (Big New Oil Initiative, 2003 – 2007; Offshore Energy Security Program, 2006 – 2011), Geoscience Australia obtained pre-competitive geoscience data to aid assessments of the petroleum prospectivity and seabed environments of the Capel and Faust basins, two under-explored basin provinces that lie offshore eastern Australia about 800 km east of Brisbane. In late 2006 and early 2007, these initiatives supported two marine cruises (surveys GA-302 and GA-2436) that acquired new seismic reflection, swath bathymetry and potential-field (gravity and magnetic) data over the Capel and Faust basins. These new data add to limited amounts of pre-existing data and greatly enhance opportunities for improving the understanding of basin provinces in the eastern extremity of Australia's marine jurisdiction.

This record describes the potential-field (gravity and magnetic) data available in the vicinity of the Capel and Faust basins and the integration of new data collected during the GA-302 and GA-2436 surveys with pre-existing ship-track data. Given the often sparse coverage of ship-track gravity and magnetic data, global gravity and magnetic datasets, derived externally to Geoscience Australia, are also described. These global datasets have the advantage of uniform coverage of the Capel/Faust region, but at limited resolution and accuracy. Despite the limitations, these data are nevertheless useful for placing detailed interpretations of the Capel and Faust basins within a regional context.

A key step in processing ship-borne gravity and magnetic data is to “level” the data in order to minimise mis-tie errors at ship-track cross-overs. Without accounting for these cross-over errors, gridded data can be rendered un-interpretable by artefacts and distortions at line cross-overs. The ship-track data described in this record were levelled using tools within the INTREPIDTM software package and a workflow previously used by Geoscience Australia to level Australian ship-track data. Gravity data were levelled using a polynomial misfit function and a reference surface based on gravity data derived from satellite radar altimeter measurements. Magnetic data were levelled using standard loop-levelling techniques. Data preparation involved splitting tracks into relatively straight-line segments (to aid the levelling process), some filtering to smooth older data and editing to remove lines with spurious data or lines that lay close to other lines.

The levelled gravity and magnetic data are provided on a CD-ROM with this record. The data provided include:

- line-based data (both levelled and un-levelled),
- grids of free-air, simple Bouguer and band-pass filtered simple Bouguer gravity anomalies,
- grids of total-field, reduced-to-pole and band-pass filtered reduced-to-pole magnetic anomalies.

These data provide comprehensive coverage of the Capel and Faust basins in the region enclosing 157–165°E/24–31°S.

1 Introduction

The Capel and Faust basins (Stagg et al., 1999) are located offshore eastern Australia, about 800 km east of Brisbane in 1000–3000 m of water (CB and FB in Figure 1.1). They are part of the Lord Howe Rise, a continental ribbon that separated from the Australian continent during Cretaceous rifting and opening of the Tasman Sea (Gaina et al., 1998; Norvick et al., 2001; Willcox et al., 2001; Norvick et al., 2008). Prior to 2006, definitive geological constraints on the architecture and makeup of the Lord Howe Rise region were limited to a small number of relatively shallow Deep Sea Drilling Program (DSDP) drill holes, dredge samples and seismic lines (e.g. Stagg et al., 2002; Willcox and Sayers, 2002; van de Beuque et al., 2003).

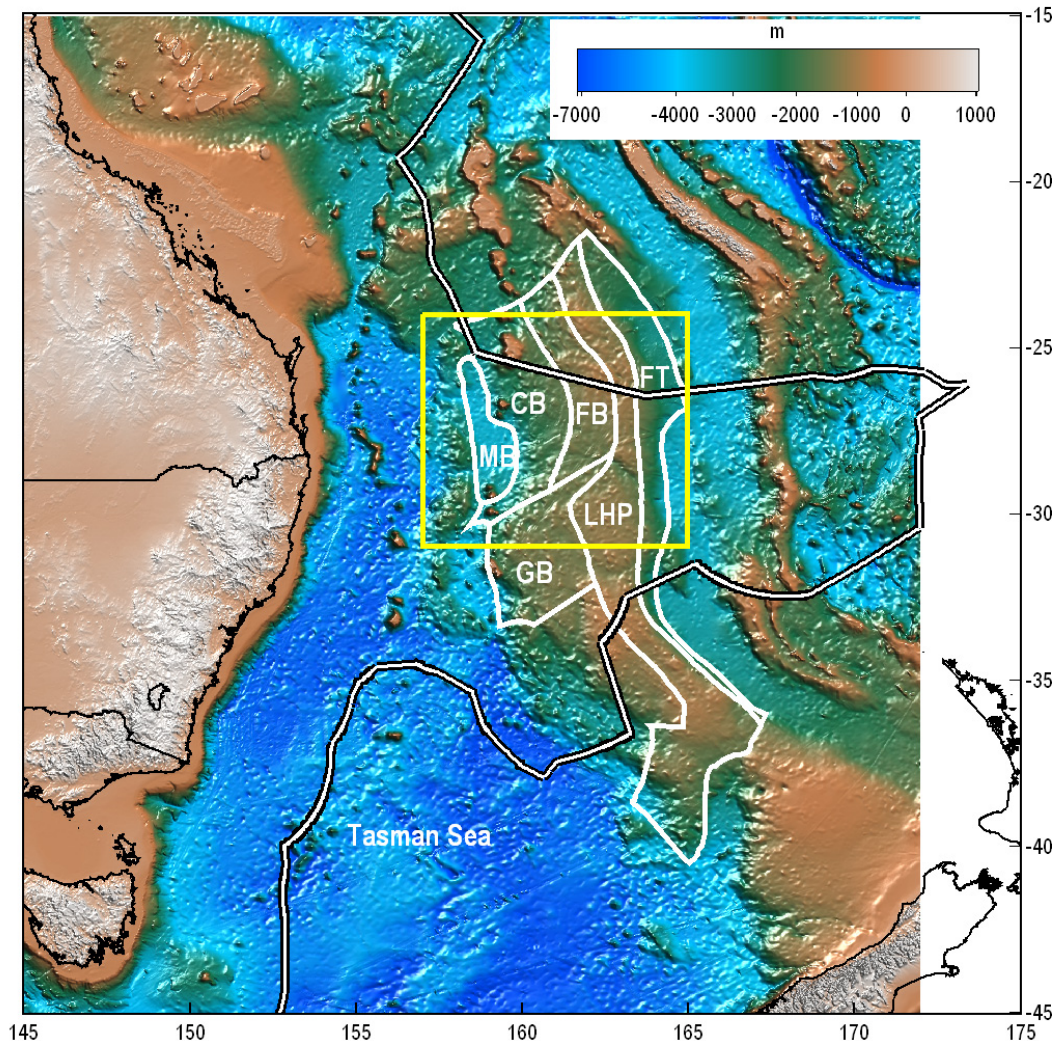


Figure 1.1: Map showing bathymetry (depth in m) of the eastern Australian region from the 2009 Bathymetry and Topography Grid of Australia (Whiteway, 2009) together with the outline of the main tectonic elements of the northern Lord Howe Rise (as defined by Stagg et al., 1999): CB, Capel Basin; FB, Faust Basin; MB, Middleton Basin; GB, Gower Basin; LHP, Lord Howe Platform; FT, Fairway Trough. The yellow box encloses the GA-302 seismic reflection and GA-2436 swath mapping surveys and outlines the area in which ship-track potential field data were collated and levelled. The white-on-black line shows the outer limit of Australia's continental shelf (seabed) jurisdiction as defined by the UN convention on the Law of the Sea and certain treaties (not all in force).

Relatively little is known about the Capel and Faust basins. The basin outlines were defined on the basis of regional reconnaissance seismic lines (Stagg et al., 1999) and satellite-derived gravity anomalies. The satellite-derived gravity anomalies, with their complete regional coverage (but relatively low resolution), enable the identification of tectonic domains and can also be used to assist modelling of the tectonic evolution of the eastern Australian margin (van de Beuque et al., 2003; Norvick et al., 2008).

Studying the Capel and Faust basins has received new impetus as the result of a need to better understand the geology, resource potential and seafloor environments of the remote, easternmost parts of Australia's marine jurisdiction. As part of two major Australian Government initiatives (Big New Oil Initiative, 2003–2007; Offshore Energy Security Program, 2006–2011), two marine geoscience cruises were conducted over the southern parts of the Capel and Faust basins in late 2006 and 2007. These cruises, identified as surveys GA-302 and GA-2436, were aimed to provide pre-competitive geoscience data to aid assessments of the basin's petroleum prospectivity and seabed environments (Heap et al., 2009; Hashimoto et al., 2010).

The GA-302 and GA-2436 surveys provided 5920 km of new seismic reflection data, swath bathymetry data and about 17 000 line km of new gravity and magnetic data (Kroh et al., 2007; Hashimoto et al., 2008; Heap et al., 2008). The key aspects of the marine surveys are documented in contractor reports (Fugro-Robertson, 2007; Fugro-Seismic, 2007; Fugro-Robertson, 2008) and cruise reports (Heap et al., 2009). The interpretation of the seismic reflection data is described by Colwell et al. (in press).

This record describes the potential field data acquired as part of the GA-302 and GA-2436 surveys as well as its integration with pre-existing potential field data. The potential field data have aided the process of extrapolating structures interpreted in the seismic data between the relatively widely-spaced (20–50 km) lines (Hackney et al., 2009; Higgins et al., in prep.; Colwell et al., in press) and provide important constraints on three-dimensional modelling to ascertain total sediment thickness (Petkovic et al., 2010; in prep.).

The data described in this record lie primarily within the immediate vicinity of the GA-302 seismic reflection lines (157–165°E, 24–31°S, yellow box in [Figure 1.1](#)). However, regional gravity and magnetic datasets – sourced externally to Geoscience Australia – covering the region enclosing eastern Australia, the Tasman Sea, Lord Howe Rise, New Zealand and New Caledonia ([Figure 1.1](#)) are also described. These data provide a means to place interpretations of the Capel and Faust basins within a regional context.

2 Existing data

Prior to the GA-302 and GA-2436 marine surveys, there was limited potential field data covering the Capel and Faust basins. However, existing regional data that partly covers the Capel and Faust basins include satellite-altimetry derived global gravity datasets, global compilations of magnetic data and some ship-track data. These datasets are summarised below.

2.1 SATELLITE-DERIVED GRAVITY DATA

Gravity anomalies for the world's oceans at wavelengths less than about 400 km can be determined from radar altimetry measurements of ocean surface slope made from satellites (Sandwell and Smith, 1997; Fairhead et al., 2001; Andersen et al., 2010b). The ocean-surface slope effectively gives the slope of the geoid, the equipotential surface that best fits mean sea level. Gravity anomalies can be derived from the derivative of potential, so knowledge of ocean-surface (geoid) slope can be used to compute gravity anomalies (see, for example, Sandwell and Smith, 1997).

The surface slope measurements are determined by differencing radar-based height measurements along satellite tracks. The height measurements themselves are derived by "tracking" the raw radar altimeter waveforms returned to the satellite. Tracking involves a process of modelling the waveforms in terms of signal amplitude, decay rate and, most importantly, the signal arrival time. The arrival time of the reflected signal provides the height measurement, but the exact arrival time for the point on the sea surface nearest the satellite is obscured by the multitude of reflections returning from the broad footprint of the radar pulse (Sandwell et al., 2001).

Waveform tracking can be done in real time onboard the satellites, resulting in radar range accuracies of 30–40 mm that in turn lead to gravity field accuracies of 40–60 $\mu\text{m/s}^2$ (Sandwell and Smith, 2009). Re-tracking the waveforms at a later stage can improve accuracy to around 20–30 $\mu\text{m/s}^2$.

The main limitation of the altimeter derived datasets is their spatial resolution, which is limited to ~16–25 km (Louis et al., 2010). This limitation is the result of the spacing between satellite tracks and the filtering required to suppress noise induced by factors such as the roughness of the ocean surface caused by waves (e.g. Sandwell et al., 2001). This wave-induced noise can be reduced by making repeat measurements.

Two satellite-altimetry-derived gravity datasets are available: those provided from the Scripps Institution of Oceanography¹ and those from the Danish National Space Centre². Each is briefly described below.

2.1.1 Datasets from Scripps Institution of Oceanography

The most commonly used global marine satellite derived gravity datasets are those from the Scripps Institution of Oceanography (hereafter referred to as the SIO datasets). Version 7.2, based on data from the Geosat and ERS-1 satellites, was the original version of the dataset with almost global coverage (Sandwell and Smith, 1997). Several versions have since been released, the most recent of which is version 18.1 (Sandwell and Smith, 2009). The newer datasets do not include new radar altimeter measurements – accuracy improvements are achieved purely by re-tracking existing waveform data and through the use of better geoid models during processing. Older datasets were provided with a spatial resolution of two arc minutes (2'), whereas V18.1 is provided at 1' (~1.8 km) resolution in order to retain the higher spatial resolution provided by the re-tracked data. Version 16.1 free-air anomalies, used for planning the GA-302 seismic reflection survey (Kroh et al., 2007), are shown in [Figure 2.1](#).

¹ http://topex.ucsd.edu/WWW_html/mar_grav.html

² http://www.space.dtu.dk/English/Research/Scientific_data_and_models/Global_Marine_Gravity_Field.aspx

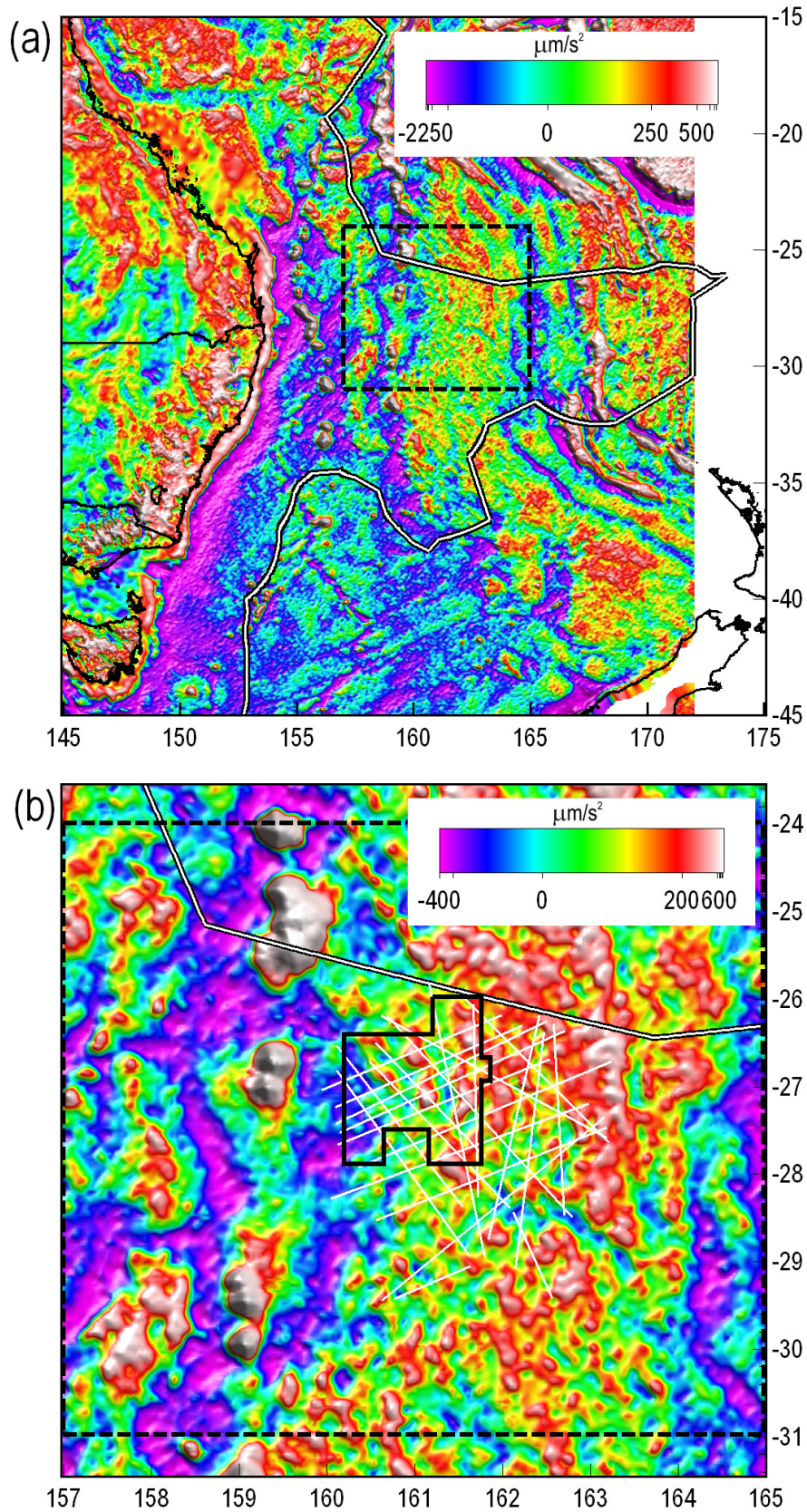


Figure 2.1: Maps of Scripps Institution of Oceanography (SIO) V16.1 satellite altimetry derived free-air gravity (in $\mu\text{m/s}^2$) for (a) the eastern Australian region and (b) the southern parts of the Capel and Faust basins. The dashed box outlines the area in which ship-track potential field data were collated and levelled and the white-on-black line is the limit of Australia's marine jurisdiction (see Figure 1.1 for details). The white lines in (b) show survey GA-302 seismic reflection lines and the black polygon outlines survey GA-2436.

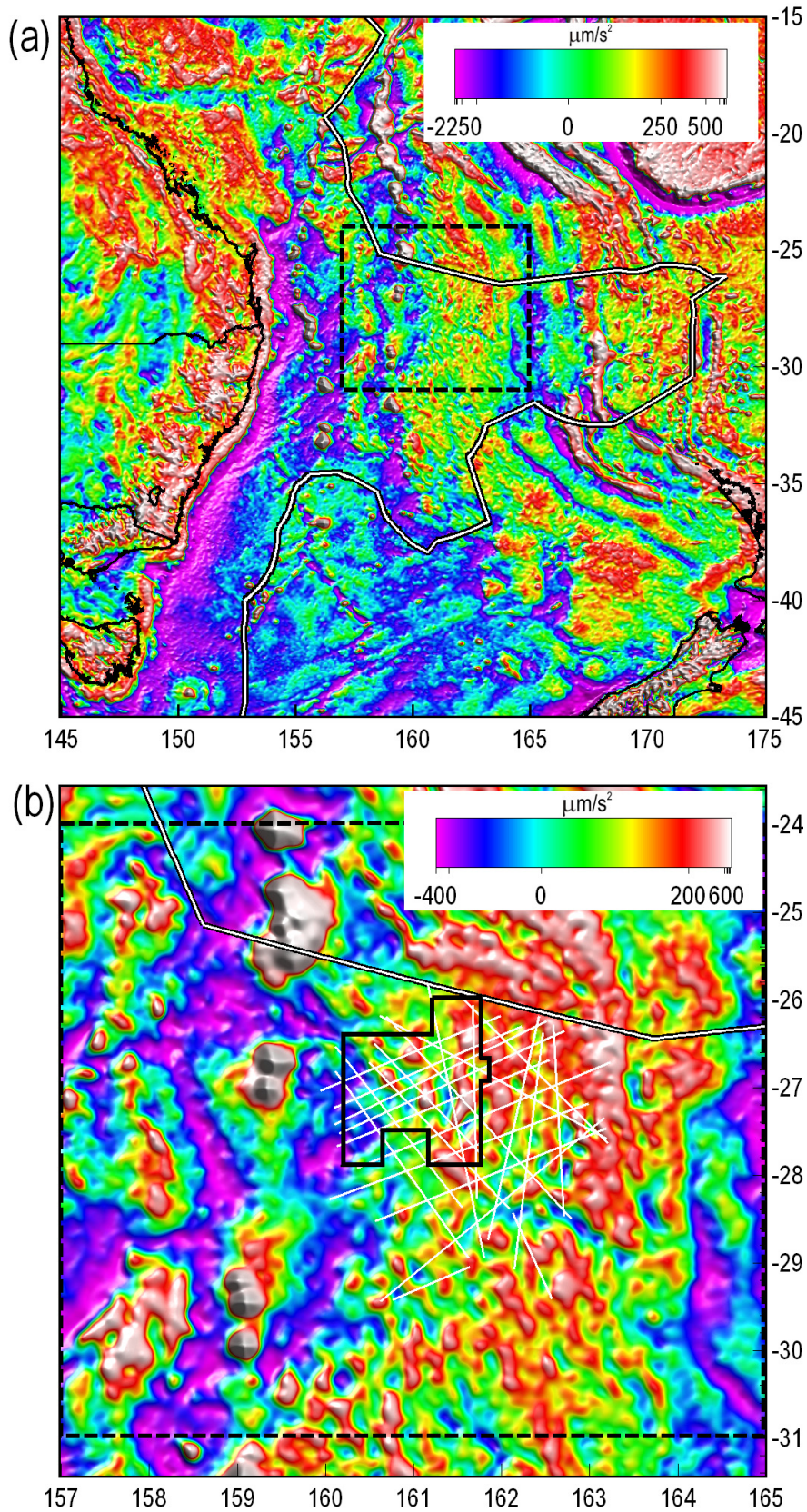


Figure 2.2: Maps of free-air gravity anomalies (in $\mu\text{m/s}^2$) from the DNSC08GRA satellite-altimetry dataset for (a) the eastern Australian region and (b) the Capel/Faust region. The dashed box outlines the area in which ship-track potential field data were collated and levelled and the white-on-black line is the limit of Australia's marine jurisdiction (see Figure 1.1 for details). The white lines in (b) show survey GA-302 seismic reflection lines and the black polygon outlines survey GA-2436.

Sandwell and Smith (2009) provide an assessment of the accuracy of the various SIO gravity datasets derived from Geosat/ERS-1 radar measurements. With each new model, the noise level has decreased and a comparison with selected shipboard measurements shows improvements in accuracy between earlier (V9.1) and most recent (V18.1) datasets of up to 46%. In general, comparisons between V18.1 and shipboard measurements agree to within 25–35 $\mu\text{m/s}^2$, whereas comparisons using V9.1 show larger differences of up to 50–60 $\mu\text{m/s}^2$ (Sandwell and Smith, 2009). In areas with large, narrow and high-relief seafloor features (e.g. seamounts), mismatches can reach 200 $\mu\text{m/s}^2$.

The seismic lines for survey GA-302 were planned on the basis of version 16.1 of the Geosat/ERS-1 data (Kroh et al., 2007). These data highlighted prominent negative gravity anomalies with wavelengths of 50–100 km (Figure 2.1b) that correlated with sediment depocentres evident in older seismic data (e.g. van de Beauque et al., 2003). The new seismic survey (GA-302) was planned to cross the most prominent negative anomalies evident in the V16.1 satellite altimeter data.

2.1.2 Datasets from the Danish National Space Centre

The Danish National Space Centre has released DNSC08GRA, a global satellite-altimetry derived dataset of free-air gravity anomalies (Andersen et al., 2010a) (Figure 2.2). Like the SIO datasets, DNSC08 is also based on re-tracked Geosat and ERS-1 data, but it also incorporates waveform data from additional satellites (e.g. IceSAT, Topex/Poseidon, Jason-1, ERS-2). Also, the DNSC08 data give a more accurate representation of gravity anomalies near the coastline (i.e. within ~200 km of the coast) where radar waveforms are influenced by near-shore currents and degraded by the interruption of the radar footprint caused by overlap onto land. By incorporating IceSAT data, the DNSC08 dataset extends to polar regions – the Geosat and ERS-1 datasets are limited to the latitude range of $\pm 72^\circ$, a consequence of the orbit inclination of the satellites.

The DNSC08 data are an improvement on the SIO data used to plan the GA-302 seismic survey. The newer datasets are provided at a higher resolution (one arc minute) that is generally suitable in its own right for regional tectonic interpretations and even for the interpretation of basin location on the Lord Howe Rise. However, using gravity data for interpretation of upper-crustal structure requires the removal of the gravitational effects of bathymetry variations and long-wavelength effects related to deeper crustal structure and the Moho. For this purpose, the DNSC08GRA free-air anomalies (Figure 2.2) were converted to simple Bouguer anomalies using GEBCO 1' bathymetry (see Section 3) and a Bouguer correction density of 970 kg/m^3 (the difference between water density and assumed rock density; 1030 kg/m^3 and 2000 kg/m^3 , respectively). Long-wavelength effects were accounted for by subtracting a regional field computed by upward continuing the Bouguer gravity by 25 km (cf. Kroh et al., 2007; Morse, 2010). Figure 2.3 shows the resulting residual gravity map for the eastern Australian region. This map highlights the alternating negative/positive anomalies with wavelengths of 50–100 km that characterise much of the Lord Howe Rise.

2.2 GLOBAL COMPILATIONS OF MAGNETIC DATA

In recent years there has been considerable effort directed towards compiling global maps of magnetic anomalies. These efforts culminated in the release of the World Digital Magnetic Anomaly Map (WDMAM) in 2007 (Korhonen et al., 2007; Maus et al., 2007). This map combines magnetic data from airborne and marine surveys and from the CHAMP satellite. In areas of sparse marine data, synthetic magnetic anomalies computed from seafloor age were included. The WDMAM data are provided at 5 km above mean sea level (geoid) with a resolution of three arc minutes (3').

An updated version of the dataset used to produce the WDMAM has been released as Earth Magnetic Anomaly Grid 2, EMAG2³ (Maus et al., 2009). This dataset incorporates data from newer land and marine surveys (notably for the Australian margins) and, for wavelengths longer than 330 km, data from the latest CHAMP lithospheric magnetic field model (MF6, Maus et al., 2008). Instead of using synthetic anomalies in marine areas with poor data coverage, the age of the ocean floor was used to guide advanced directional-gridding methods to allow extrapolation into the data poor areas. EMAG2 provides global anomalies at

³ <http://www.geomag.us/models/emag2.html>

4 km above the geoid and with a 2' resolution (Maus et al., 2009). Despite the limited resolution, the EMAG2 dataset is a useful aid to regional interpretation of structure and tectonics within the eastern Australian region. EMAG2 data for the eastern Australian region are shown in [Figure 2.4](#).

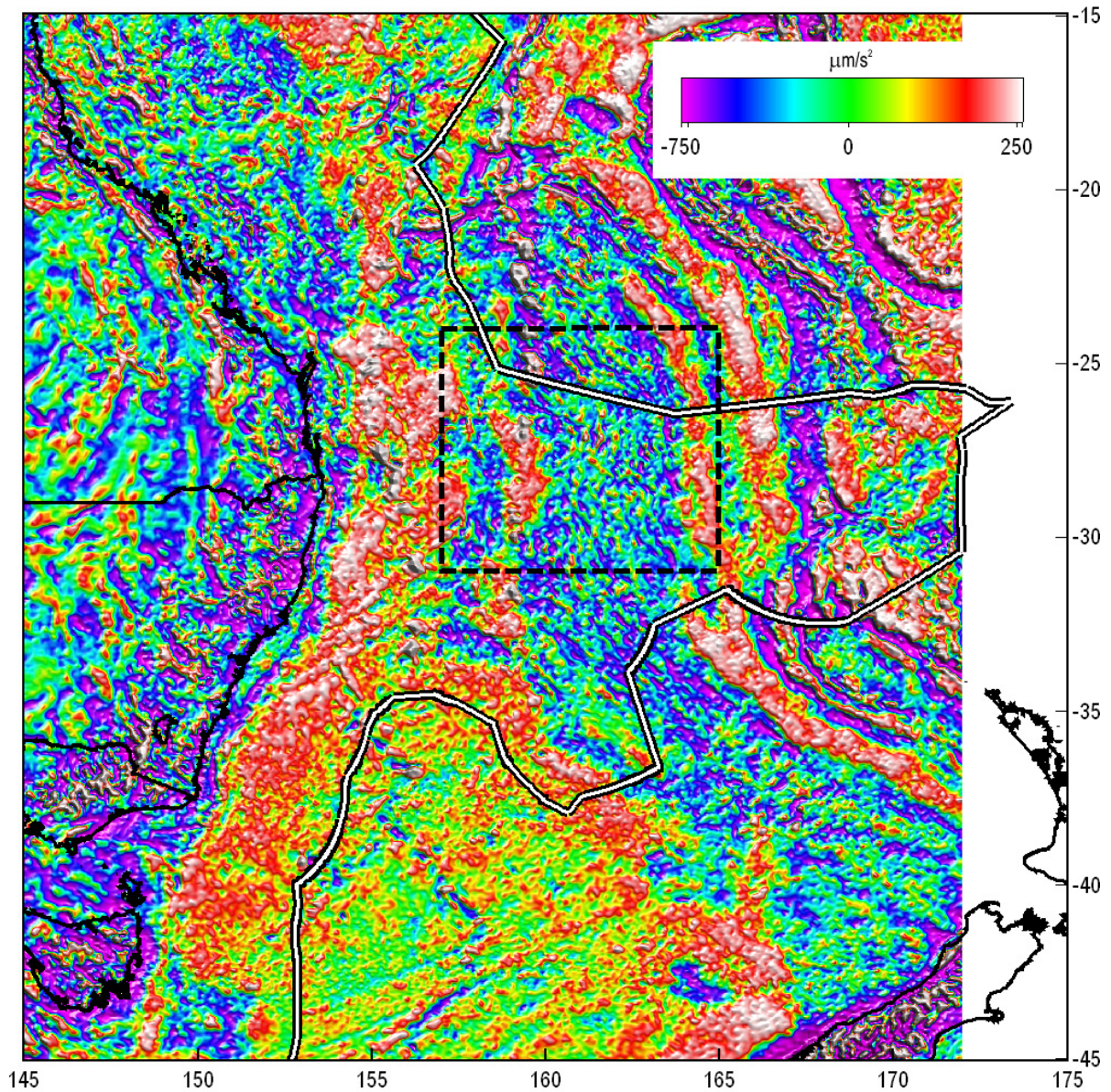


Figure 2.3: Map showing residual Bouguer gravity (in $\mu\text{m/s}^2$) for the eastern Australian region derived from DNSCO8 data. The simple Bouguer gravity (i.e. without terrain corrections) was computed using an infinite-slab Bouguer correction with a density contrast relative to seawater of 970 kg/m^3 . The subtracted regional field was computed by upward continuing the Bouguer gravity to 25 km. The dashed line outlines the area in which ship-track potential field data were collated and levelled and the white-on-black line is the limit of Australia's marine jurisdiction (see [Figure 1.1](#) for details).

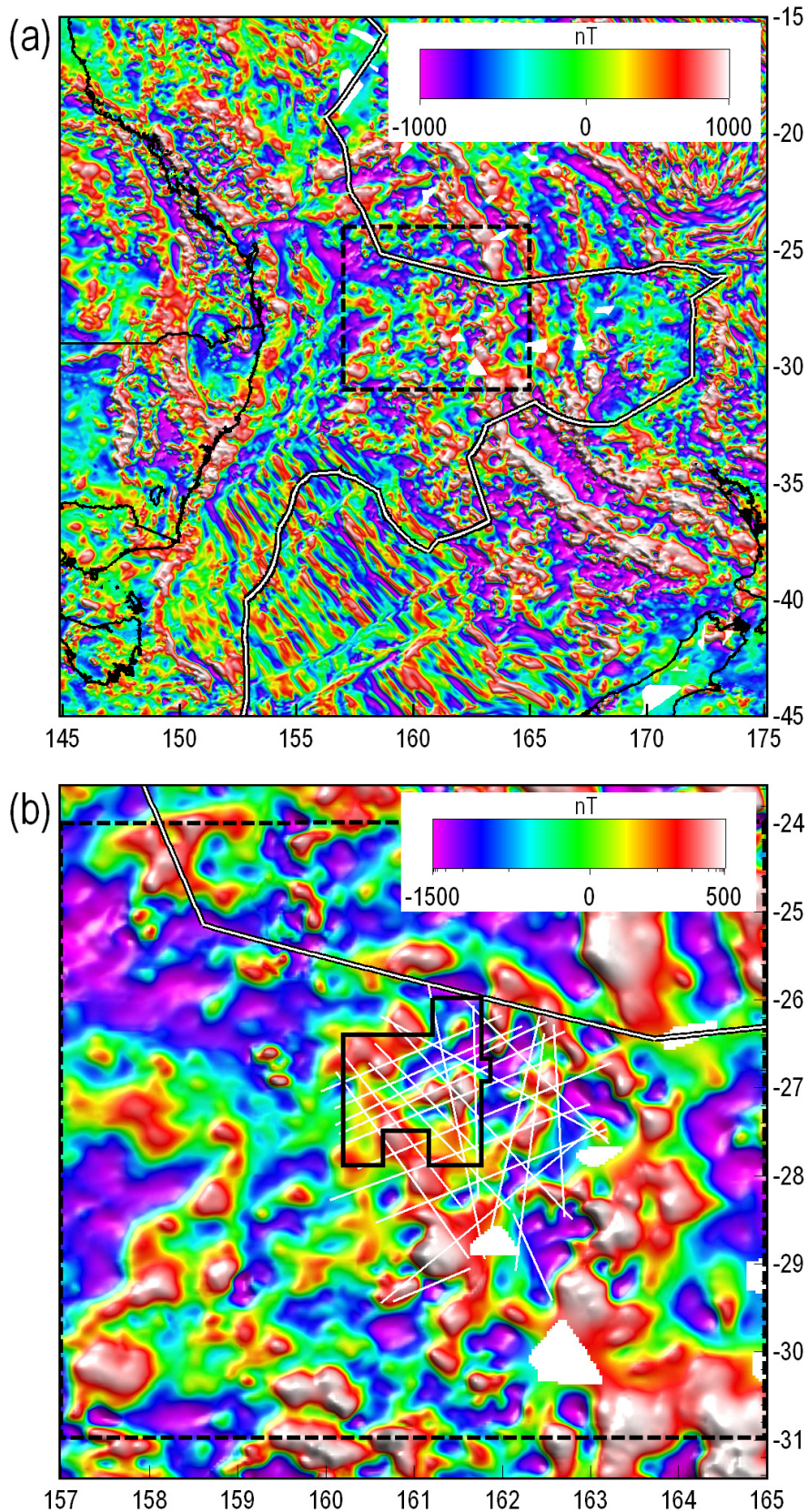


Figure 2.4: Map showing magnetic anomalies (in nT) from the EMAG2 dataset (Maus et al., 2009) for (a) the eastern Australian region and (b) the Capel/Faust region. The dashed box outlines the area in which ship-track potential field data were collated and levelled and the white-on-black line is the limit of Australia's marine jurisdiction (see Figure 1.1 for details). The white lines in (b) show survey GA-302 seismic reflection lines and the black polygon outlines survey GA-2436.

2.3 MARINE DATA

Marine potential field data are important for geological interpretation because they are measured at the surface with higher resolution than is possible from space-based measurements. However, resolution is only high along the ship-tracks themselves and anomalies from underlying geology are also attenuated as a result of the water column, especially in deep-water areas. In addition, ship tracks are generally widely separated, meaning that achieving spatially-complete gravity and magnetic anomaly coverage is limited by the need to interpolate between widely-separated data points. Marine gravity and magnetic data must also be “levelled” so that often-substantial misfits at ship-track crossovers are removed or minimised.

In some applications, shipboard measurements of the gravity field are being surpassed by the latest satellite-altimeter derived gravity data (e.g. Fairhead et al., 2001). For many purposes, particularly in frontier regions, the current resolution achievable with satellite altimetry is sufficient to aid in mapping out gross-scale basin geometry and regional tectonic fabric. Nevertheless, marine measurements of gravity and magnetic data are the only way to achieve high resolution data in areas of particular interest. Without marine measurements, global compilations such as EMAG2 would not be possible and global maps of magnetic anomalies would be limited to the inherently long-wavelengths (>330 km) provided by satellites like CHAMP.

Geoscience Australia holds a large dataset of marine gravity and magnetic data, a large part of which has been previously levelled. This section describes marine data that were available in the Capel/Faust region prior to the most recent Geoscience Australia surveys.

2.3.1 Levelled marine data

The sparsity of data in many areas around the Australian margin means that levelling the marine gravity and magnetic data is difficult. Featherstone (2009) attempted a classical least-squares adjustment of marine gravity data, but concluded that accurate levelling was not possible due to the low number of ship tracks and their wide separation.

Geoscience Australia's holding of bathymetry and marine potential-field data up to 2001 was levelled using methods developed by INTREPID GEOPHYSICS under contract to Geoscience Australia (DFA, 2001; Petkovic et al., 2001) (Figure 2.5). Marine magnetic data were levelled using a loop-adjustment technique, whereas the gravity data were levelled using a polynomial misfit function derived from crossover misfits between the marine ship-tracks and V9.2 of the SIO satellite-altimetry derived data. This approach is subject to the limitations of satellite-altimetry-derived data in coastal regions, continental shelves and shallow seas where altimeter range corrections for tides and atmospheric effects are poor (e.g. Andersen and Knudsen, 2000; Deng and Featherstone, 2006; Hwang et al., 2006). For this reason, the satellite-derived reference surface was not used in some areas (e.g. Bass Strait). Figure 2.6 shows the 2001 levelled marine data over the Capel and Faust basins.

The free-air anomalies, δg_F , in the levelled dataset were computed using

$$\delta g_F = g_{obs} - \gamma \quad (1)$$

where g_{obs} is the measured gravity and γ is normal gravity on the reference ellipsoid. Measurements are assumed to have been made at sea level, meaning that any separation between the geoid (mean sea level) and the reference ellipsoid has not been taken into account. Normal gravity in this dataset was computed from:

$$\gamma = \gamma_e (1 + \alpha \sin^2 \phi - \beta \sin^2(2\phi)) \quad (2)$$

where γ_e is normal gravity at the equator, ϕ is latitude and α and β are parameters related to the form of the reference ellipsoid (assumed to be WGS84).

Despite the challenges posed when combining and levelling a diverse set of marine potential field data collected over several decades, it is possible to derive meaningful datasets that are useful for geological and tectonic interpretations. This is demonstrated by the EMAG2 dataset (Section 2.2) and by a comparison between the 2001 levelled marine gravity data (Petkovic et al., 2001) with the DNSC08GRA satellite altimetry derived gravity anomalies. Except in some coastal regions, the 2001 levelled dataset compares well with the DNSC08GRA data (Figure 2.7). The biggest differences in coastal regions probably reflect the fact that the polynomial levelling technique used by Intrepid Geophysics was referenced to V9.2 of the Sandwell and Smith satellite gravity dataset, which is not as accurate near the coast as more recent datasets.

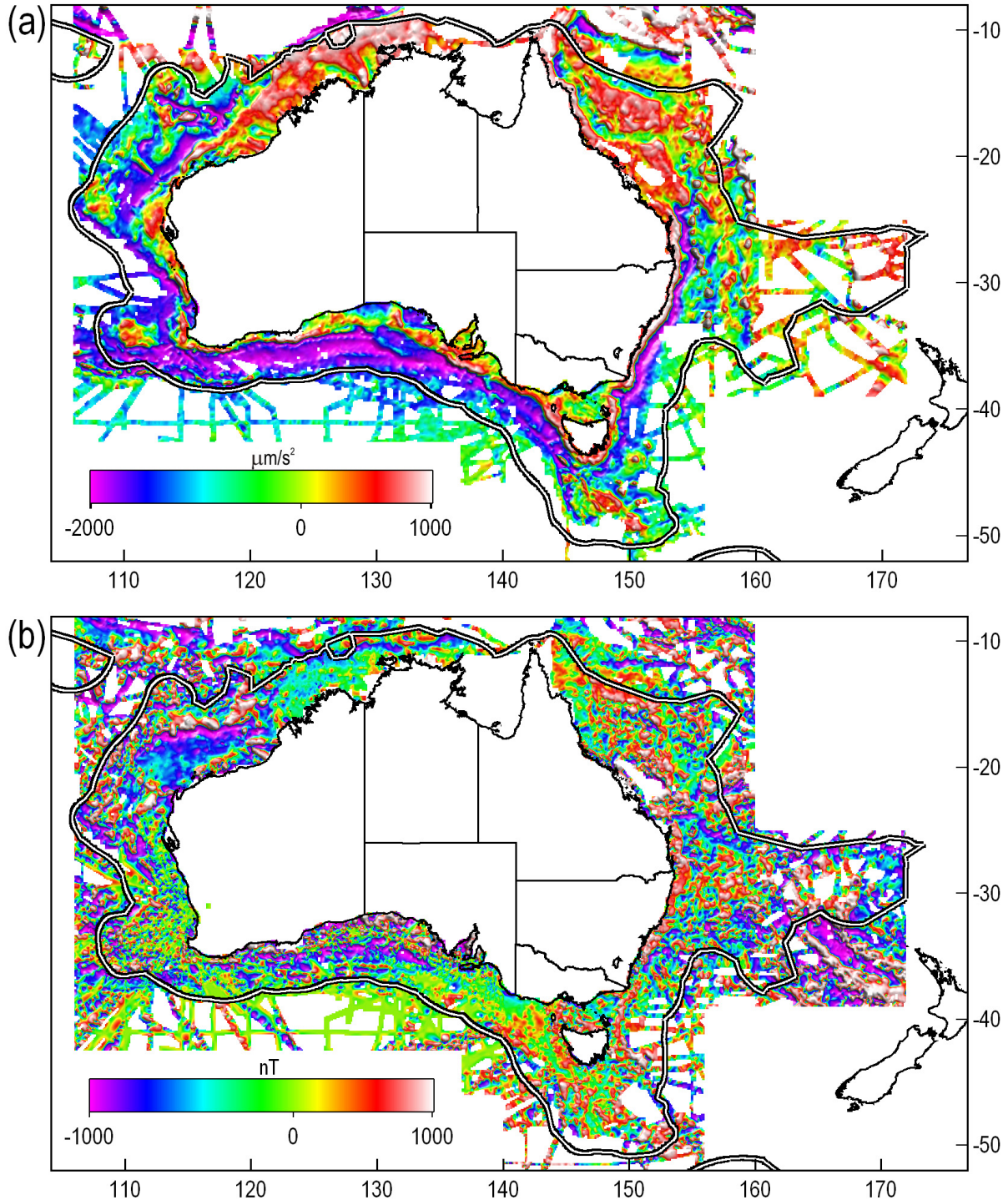


Figure 2.5: Maps showing grids (0.1° cell-size, ~ 10 km) of (a) levelled gravity data ($\mu\text{m/s}^2$) and (b) levelled magnetic data (nT) for the marine areas around Australia (Petkovic et al., 2001). The white-on-black line is the limit of Australia's marine jurisdiction (see Figure 1.1 for details).

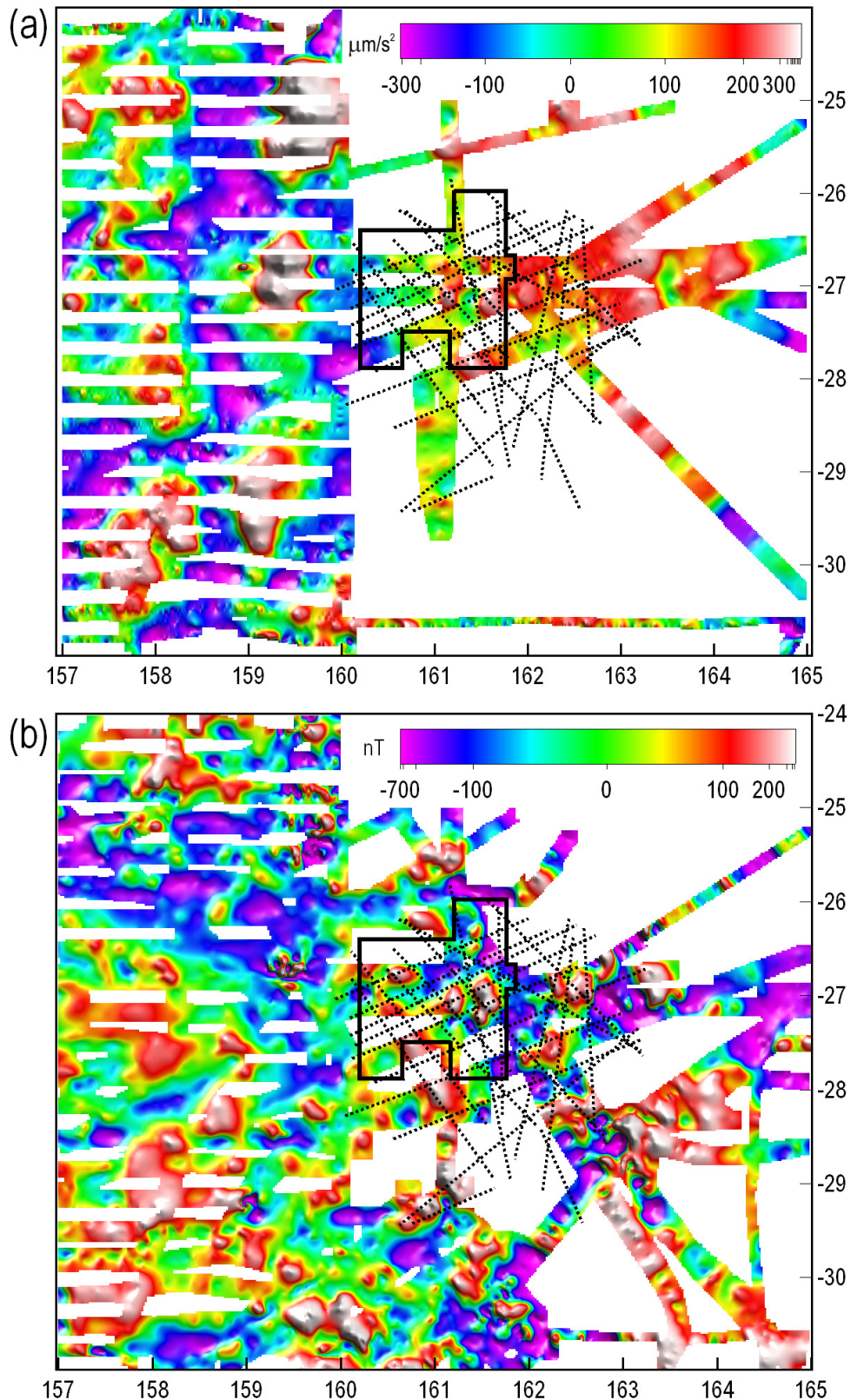


Figure 2.6: Maps showing the previously-levelled marine (a) gravity ($\mu\text{m/s}^2$) and (b) magnetic (nT) data over the southern parts of the Capel and Faust basins (Petkovic et al., 2001). Note that data from the more recent GA-302 (dashed lines) and GA-2436 (black polygon) surveys were not included in this earlier levelling.

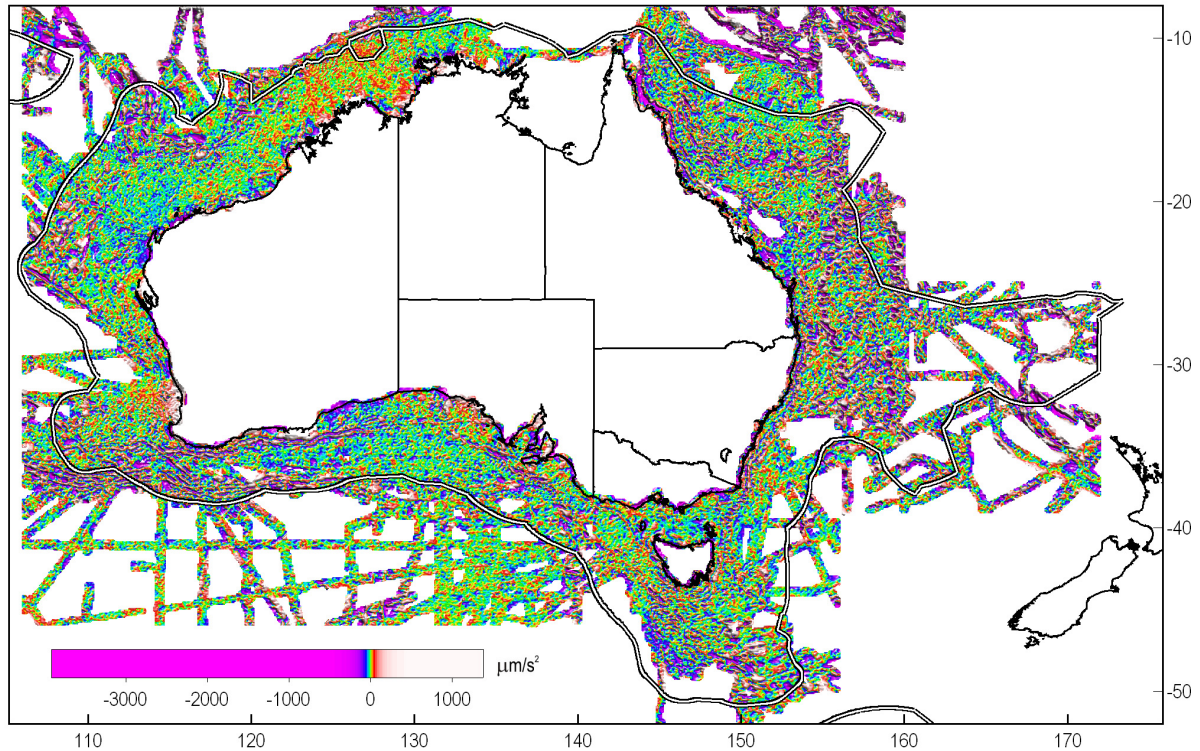


Figure 2.7: Differences between the 2001 levelled marine gravity dataset and DNSC08GRA free-air gravity anomalies (in $\mu\text{m/s}^2$). The map shows that the levelled marine data match the DNSC08 data to within about $\pm 100 \mu\text{m/s}^2$ (mean difference $-1.9 \mu\text{m/s}^2$, standard deviation $112 \mu\text{m/s}^2$). The white-on-black line is the limit of Australia’s marine jurisdiction (see [Figure 1.1](#) for details).

2.3.2 Post-2001 marine surveys

The dataset of levelled marine potential field data described above has not been updated since 2001. Since then, many new surveys have been conducted, but these surveys have not been levelled with the existing dataset. This is despite the fact that most of these surveys have been levelled on an individual basis (i.e. “internally” levelled) by the contractors supplying the data.

In the time since the Australian marine potential field data were last levelled, only five new surveys with potential field data have been conducted over the southern Capel and Faust basins. These are surveys GA-270, GA-1892, GA-2311, GA-302 and GA-2436. The latter two surveys were designed specifically to target the Capel and Faust basins and potential field data from these two surveys are described in the next section. Data from the remaining three surveys have not been incorporated into the new Capel/Faust potential field database for the reasons outlined in Table 1.

Table 1: Marine surveys in the Capel/Faust area ($157\text{--}165^\circ\text{E}$, $24\text{--}31^\circ\text{S}$) conducted between the time that marine potential field data were last levelled (Petkovic et al., 2001) and the most recent surveys of the Capel and Faust basins (GA-302 and GA-2436). The table shows the data available and the reasons why they were not included in the Capel/Faust potential field database.

| SURVEY | YEAR | DATA | REASON FOR NON-INCLUSION |
|---------|------|---------------------------|---|
| GA-270 | 2004 | Only magnetic data | Magnetic data are not corrected for receiver offset. |
| GA-1892 | 1967 | Gravity and magnetic data | Data are old and likely to be poorly positioned, further adding to levelling difficulties; Magnetic data are not corrected for receiver offset. |
| GA-2311 | 2001 | Gravity and magnetic data | Data are fully corrected and recent, but only one short line segment traverses the area covered by surveys GA-302 and GA-2436. |

3 Bathymetry data

Bathymetry data are an important part of gravity data processing because they are required for the Bouguer correction, the correction that accounts for the gravitational effect of the density contrast at the seafloor. Bathymetry is also used for the “terrain” correction that accounts the gravity effect of undulating seafloor in the region surrounding the gravity measurements.

For the purposes of processing regional data during this work, bathymetry data were taken from the 2009 Bathymetry and Topography Grid of Australia (Whitway, 2009), here referred to as AUSBATH09. AUSBATH09 is an update of the Australia-wide compilation described by Petkovic et al. (2001) and Webster and Petkovic (2005). The AUSBATH09 grid is provided at a 250 m resolution (nine arc seconds), but this resolution is only achieved in areas where shipboard bathymetry data have been measured. In areas lacking high resolution shipboard data, the global ETOPO1 dataset is used. Like the global datasets of marine free-air gravity anomalies, ETOPO1 is derived from satellite radar altimetry data using methods described by, for example, Smith and Sandwell (1997). AUSBATH09 data for the eastern Australian region are shown in Figure 3.1a.

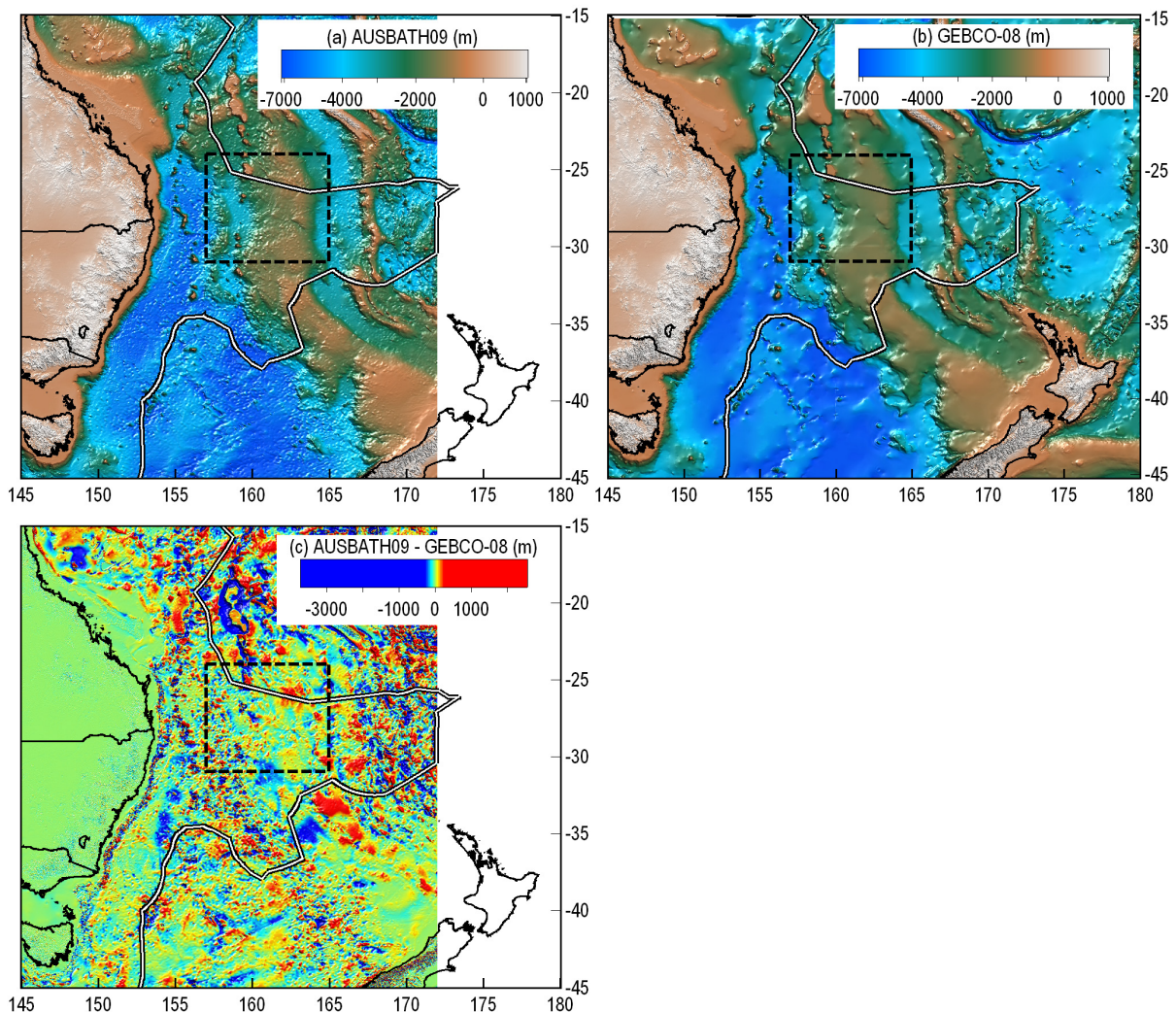


Figure 3.1: Maps showing bathymetry (depth in m) for the eastern Australian region from: (a) AUSBATH09, (b) GEBCO version 2.0 and (c) the difference between the two (mean difference -12 m; standard deviation, 203 m). The dashed line outlines the area in which ship-track potential field data were collated and levelled and the white-on-black line is the limit of Australia's marine jurisdiction (see Figure 1.1 for details).

In theory, the ETOPO1 dataset should not be used to compute the Bouguer or terrain corrections to be applied to free-air anomalies in satellite-altimetry derived datasets such as DNSC08GRA. This is because both are derived from the same radar waveform data and are, therefore, correlated. An alternative is to use data from the General Bathymetric Chart of the Oceans (GEBCO)⁴.

Version 2.0 of the GEBCO dataset, released in November 2008, does not include satellite-altimetry derived data and is simply a one-arc-minute grid of a global compilation of bathymetric contours contained within the GEBCO Digital Atlas. As such, the accuracy of these maps is often poor in areas without direct measurements of bathymetry. Bathymetry for the eastern Australian region from the GEBCO 2.0 grid is shown in [Figure 3.1b](#). The difference between the AUSBATH09 and GEBCO 2.0 grids ([Figure 3.1c](#)) highlights the deficiencies of each dataset; many parts of the GEBCO dataset have spurious water depths (e.g. the area centred on 160°E/20°S), and the parts of the AUSBATH09 grid that rely only on ETOPO1 induce short wavelength “pimpling” artefacts that are typical of satellite-altimetry datasets.

⁴ <http://www.gebco.net/>

4 Capel/Faust potential-field data

Two marine surveys were conducted by Geoscience Australia in 2006 and 2007 to specifically target the southern parts of the Capel and Faust basins as part of efforts to assess the petroleum prospectivity and seabed environments of the region. These were survey GA-302, conducted in late 2006 and early 2007, and survey GA-2436 (Tangaroa survey, TAN0713) conducted in 2007 (Figure 1.1).

4.1 SURVEY GA-302

This survey was primarily aimed at acquiring seismic reflection data, but gravity and magnetic data were collected along the seismic lines (Kroh et al., 2007). The ship-tracks (seismic lines) from this survey are shown in Figure 4.1. Gravity and magnetic data were measured during the survey and subsequently processed by Fugro Robertson Inc LCT Gravity and Magnetics Division (job number 4640). Acquisition and processing details can be found in Fugro Roberston (2007), but a summary is included below.

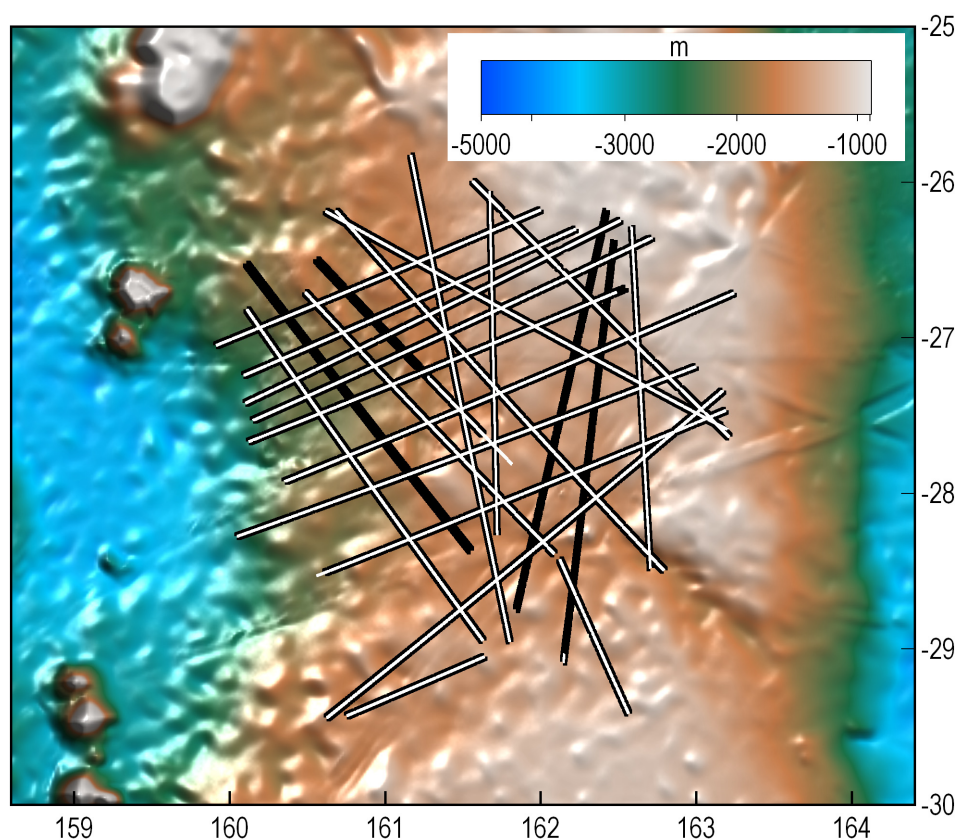


Figure 4.1: Map showing the GA-302 seismic lines along which gravity and magnetic data were collected (gravity, black lines; magnetic data, white lines; both, white-on-black lines). A 0.01° (~ 1 km) grid of the AUSBATH09 bathymetry dataset (depth in m) is shown in the background.

4.1.1 Acquisition

Gravity data were acquired using Fugro Robertson's LaCoste and Romberg air-sea gravity meter (serial number S-91). A SeaSpy Overhauser magnetometer was used to acquire the magnetic data using a sensor towed 245 m behind the ship and 12 m starboard of the centreline. Gravity, magnetic and navigation data were recorded at one second intervals.

4.1.2 Processing

After converting instrument data to raw gravity measurements, a series of standard data processing steps were applied to derive free-air gravity anomalies. These steps included: cross-correlation procedures, meter

calibration, drift correction, ties to land reference stations and correction for Earth tides and Eötvös effects. The free-air gravity anomalies were computed using modern procedures (Hackney and Featherstone, 2003; Hinze et al., 2005) that incorporate an exact equation for computing normal gravity on the reference ellipsoid, γ :

$$\gamma = \gamma_e \frac{1 + k \sin^2 \phi}{\sqrt{1 - e^2 \sin^2 \phi}} \quad (3)$$

where γ_e is normal gravity at the equator, ϕ is latitude and k and e^2 are parameters related to the form of the reference ellipsoid (GRS80 in this case).

Measurements were assumed to have been made at sea level, so application of free-air corrections was not necessary. However, given that the reference ellipsoid, to which normal gravity refers, does not coincide with mean sea level (geoid), long-wavelength gravity effects related to geoid–ellipsoid separation (cf. Hackney and Featherstone, 2003) potentially remain. Complete Bouguer anomalies were derived using a correction density of 970 kg/m³ and by applying terrain (bathymetric) corrections from a bathymetry grid compiled by Fugro Roberston that combined GEBCO data and data collected during the survey. The data were also low-pass filtered on a line-by-line basis to remove extraneous noise and then adjusted to minimise data misfits at line crossovers (i.e. internally levelled).

Magnetic data were corrected for the offset between GPS receiver and sensor and anomalies were computed by subtracting values computed from IGRF 2005 for the appropriate measurement time. The data were corrected for diurnal variations based on geomagnetic observatory data from Canberra and then internally line levelled.

4.2 SURVEY GA-2436

Survey GA-2436 (Heap et al., 2008; Heap et al., 2009) was designed as a swath mapping survey to provide high resolution swath bathymetry data in the northwestern part of the area covered during the GA-302 survey (~160–162°E; 26–28°S). This area was mapped in detail because it has the most prominent gravity anomalies and the GA-302 seismic data suggested that sediment depocentres are deepest in that area (Hashimoto et al., 2008). The GA-2436 ship-tracks are shown in [Figure 4.2](#). Fugro Roberston were also contracted to acquire and process the gravity data during the GA-2436 survey (job number 4731). Details of acquisition and processing can be found in Fugro Roberston (2008), but a summary of this report is included below.

4.2.1 Acquisition

The swath survey utilised north–south lines spaced by 3–4 km, thereby providing high-resolution gravity and magnetic data in the area of the deepest sediment depocentres. Gravity data were acquired with a LaCoste and Romberg air/sea gravity meter (serial number S-65). The type of magnetometer used is not reported in Fugro Robertson (2008), but the magnetometer was towed 210 m behind the ship. Data were sampled at one second intervals.

4.2.2 Processing

Gravity and magnetic data were processed in a similar way to those acquired during the GA-302 survey. Magnetic anomalies were computed using the tenth-generation International Geomagnetic Reference Field (IGRF-10) and diurnally corrected using data from reference stations established on Norfolk Island and in Yamba, New South Wales, on the east coast of Australia. Some of the magnetic data were affected by high-frequency noise and were subsequently low-pass filtered using a 60 second cut-off. Gravity data were also low-pass filtered on a line-by-line basis to remove noise.

Given the lack of tie lines connecting the predominantly north–south lines ([Figure 4.2](#)), additional grid-based levelling techniques were applied by Fugro Robertson in order to internally level the data. As for survey GA-302, internally adjusted and filtered free-gravity and complete Bouguer anomalies were provided along the survey lines.

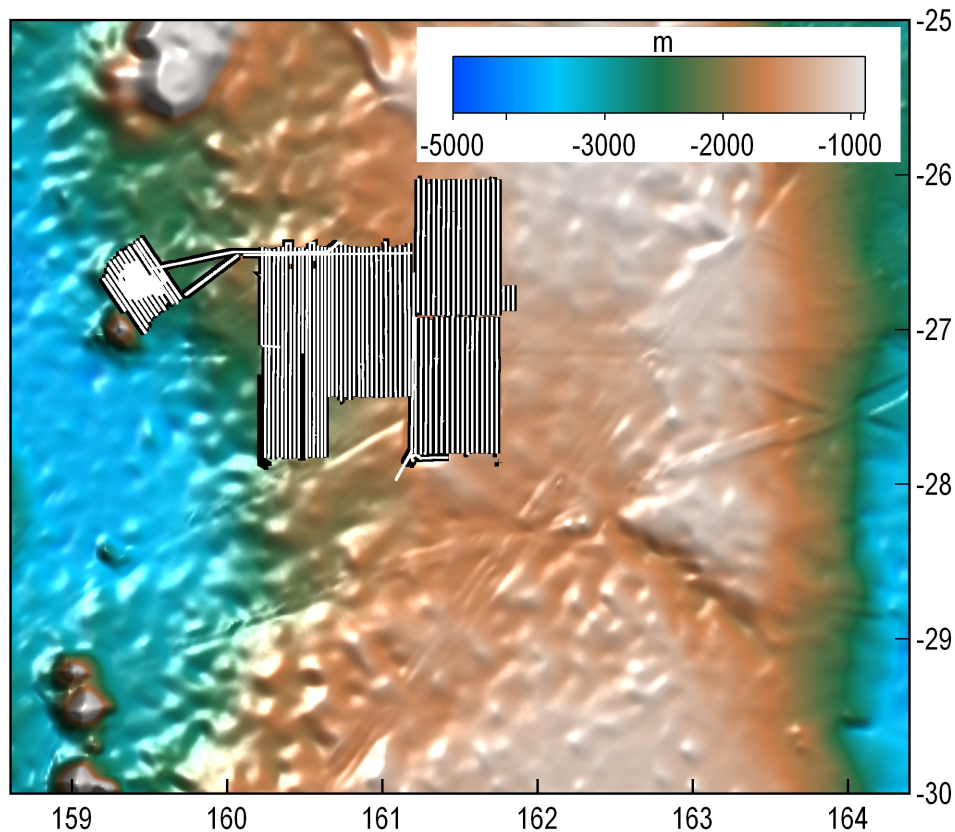


Figure 4.2: Map showing the GA-2436 survey lines along which gravity and magnetic data were collected (gravity, black lines; magnetic data, white lines; both, white-on-black lines). A 0.01° (~ 1 km) grid of the AUSBATH09 bathymetry dataset (depth in m) is shown in the background.

4.3 PRELIMINARY COMBINATION OF DATA

The GA-302 and GA-2436 gravity and magnetic data were provided by Fugro Roberston in the first half of 2008. At that stage, the provided line-based magnetic anomaly and free-air data were gridded separately using a 0.01° grid cell size. The resulting grids from the individual surveys were then merged using the INTREPID™ software. Gridded magnetic data from the previously-levelled dataset (Petkovic et al., 2001) were also merged with the GA-302 and GA-2436 data, but the gridded gravity data from that dataset did not merge well with the newer data and were excluded. Free-air gravity was then converted to simple Bouguer anomalies using a 0.01° grid of the bathymetry dataset described by Webster and Petkovic (2005). The complete Bouguer anomalies provided by Fugro Robertson were not gridded at this stage as it was intended to merge the new survey data with free-air gravity data from existing surveys and to recompute Bouguer anomalies in a consistent manner.

The merged grids of simple Bouguer and magnetic anomalies are shown in Figure 4.3. The resulting grids were further processed to aid interpretation. The magnetic data were reduced-to-pole, a process that removes the dipole nature of magnetic anomalies and essentially shifts anomalies to lie directly over their source. To aid interpretation of the seismic data (cf. Colwell et al., in press), a band-pass filter was applied to the gravity data to remove wavelengths less than 7.5 km (to smooth the grid) and greater than 100 km (to remove long-wavelength anomalies related to deeper crustal structure and the Moho). The band-pass filtered Bouguer gravity shows remarkable correlations with sediment depocentres and basement highs evident in the GA-302 seismic reflection data (e.g. Hackney et al., 2009).

The data combination described above was intended only as a preliminary effort to facilitate the interpretation process. The gravity and magnetic data described in this record are a combination of available data over the southern parts of the Capel and Faust basins that were merged at the line level. This line-based levelling is described in the next section.

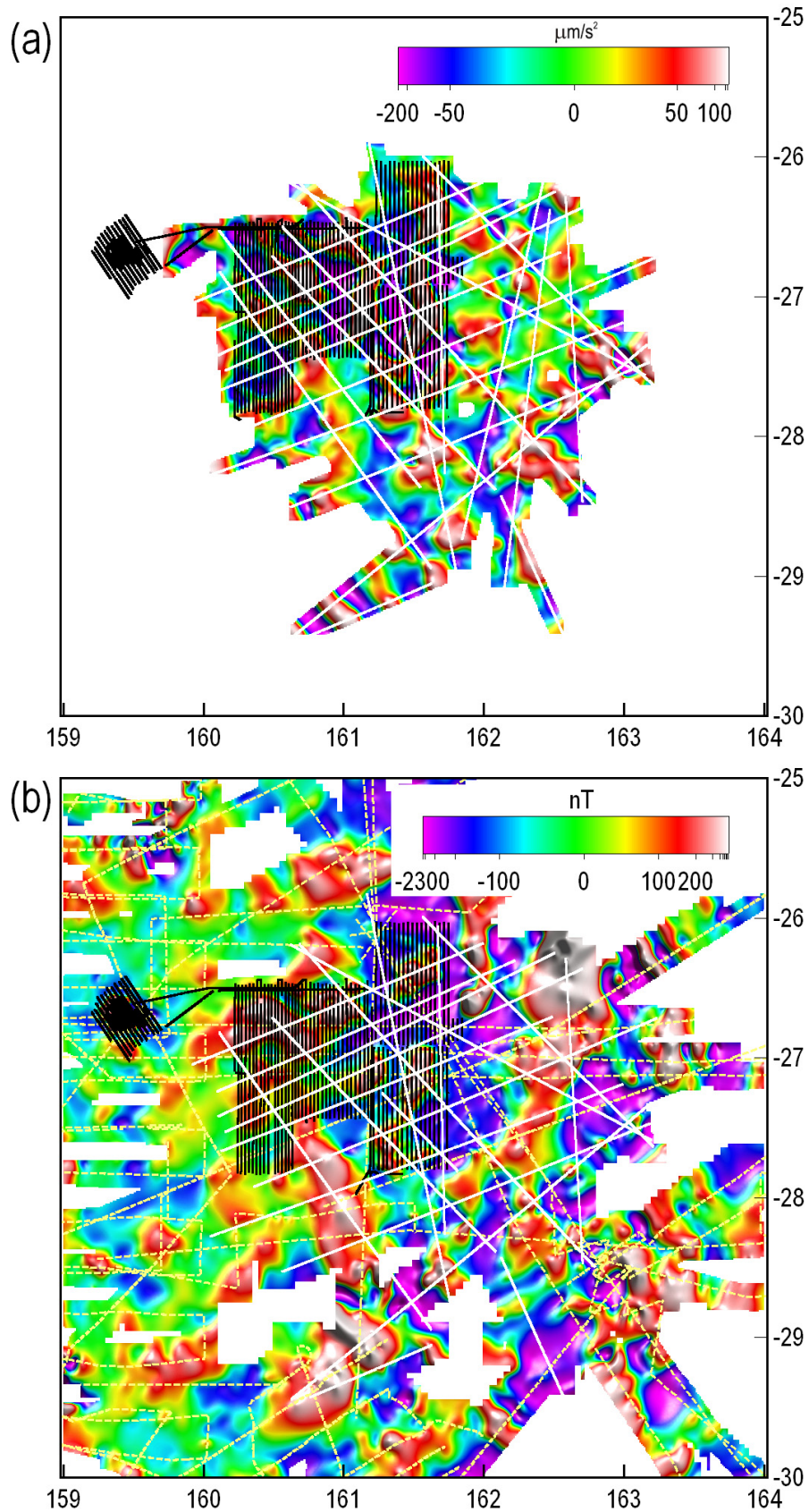


Figure 4.3: Merged grids of (a) band-pass filtered simple Bouguer anomalies ($\mu\text{m/s}^2$) and (b) reduced-to-pole magnetic anomalies (nT). Lines show the ship tracks along which data were measured (GA-302, white lines; GA-2436, black lines; other magnetic data, yellow dashed lines in b).

5 Levelled marine potential-field data

Due to the lack of an up-to-date Australia-wide dataset of levelled marine potential field data, data from the two most recent surveys of the Capel and Faust basins (GA-302 and GA-2436; [Section 4](#)) were merged and levelled together with the marine dataset described by Petkovic et al. (2001) ([Section 2.3.1](#)).

5.1 DESCRIPTION OF THE LEVELLING PROCESS

The line levelling of the datasets described above was carried out using the `marinelevel` tool in the INTREPID™ software. This tool was developed to level the line dataset described by Petkovic et al. (2001) and is described in INTREPID™ manuals and processing reports (DFA, 2001). The levelling procedure is a two-step process. The first step involves splitting lines into segments that are relatively straight and the second step levels the lines in one or more surveys using one of a variety of levelling strategies.

5.1.1 Data import

For the purposes of levelling, gravity and magnetic data from the following three datasets were imported into INTREPID™ databases:

- the part of the Australia-wide, previously-levelled dataset within an area bounded by longitudes 157 to 165°E and latitudes 31 to 24°S ([Section 2.3.1](#)),
- the GA-302 seismic survey ([Section 4.1](#)), and
- the GA-2436 swath-mapping survey ([Section 4.2](#)).

Each of these datasets was imported separately because each had a slightly different format and contained different combinations of data fields.

The existing magnetic anomaly data for each survey were imported. Gravity data required additional preparation because the free-air gravity values in the previously-levelled dataset were computed using equation (2) for normal gravity, while the GA-302 and GA-2436 free-air gravity was computed using equation (3). Therefore, observed gravity values were imported with the previously-levelled dataset and free-air anomalies were recomputed using the `gravity` tool in Intrepid. This step required selection of the appropriate gravity datum.

Intrepid gravity datums implicitly comprise a coordinate datum tied to a specific reference ellipsoid, specific formulae for calculating normal gravity, free-air corrections and Bouguer corrections, and possibly corrections for the atmosphere and geoid–ellipsoid separation. The Intrepid gravity datums relevant to this work are summarised in Table 2. It is not possible to individually select datum components (e.g. it is not possible to compute normal gravity from equation (3) using WGS84 ellipsoid parameters and then apply a correction for the geoid–ellipsoid separation).

Table 2: Summary of the properties of relevant Intrepid gravity datums

| INTREPID GRAVITY DATUM | WGS84 | GA07 |
|---|----------|----------|
| Reference ellipsoid | WGS84 | GRS80 |
| Equation for calculating γ | (3) | (3) |
| Spherical-cap Bouguer correction | optional | optional |
| Correction for geoid–ellipsoid separation | no | yes |

Observed gravity values were not provided by Fugro Robertson for the GA-302 and GA-2436 surveys. The free-air anomalies for these two datasets were computed by Fugro Robertson using equation (3) and GRS80 ellipsoidal parameters. The only gravity datum available in Intrepid that incorporates GRS80 parameters is the GA07 gravity datum. This datum also uses equation (3) to compute normal gravity and it incorporates an atmospheric correction, has the option for a spherical-cap Bouguer correction (as opposed to the infinite slab) and it also accounts for the gravity effect of the separation between the ellipsoid and geoid (the geophysical indirect effect: Hackney and Featherstone, 2003).

Given the rigid definition of gravity datums in INTREPID™, it was decided to re-compute free-air gravity for the previously-levelled dataset using the INTREPID™ WGS84 gravity “datum”. In order to avoid the need to correct for geoid–ellipsoid separation, it was assumed that the Fugro Robertson free-air gravity is also linked to the WGS84 gravity datum. This assumption is reasonable because at the scale of this work: (1) the WGS84 and GRS80 ellipsoids are essentially identical; (2) differences in the normal gravity computed using equation (3) with either GRS80 or WGS84 ellipsoidal parameters are orders of magnitude smaller than measurement errors; and (3) for areas similar in extent to the Capel/Faust basins, the errors induced by not correcting for geoid–ellipsoid separation are small (Hackney and Featherstone, 2003). Nevertheless, this correction was applied to the data before 3D modelling (Petkovic et al., 2010; in prep.).

Finally, the GA-302 and GA-2436 data were tied to the IGSN71 absolute gravity reference network during port calls and it is assumed that all data in the previously-levelled dataset were either tied directly to this reference network or corrected to be compatible with it.

5.1.2 Line splitting

The lines contained within each of the three imported datasets were generally continuous throughout the survey area (i.e. transit lines are included and there were no breaks at changes in line direction; Figure 5.1). Data recorded during changes in direction can be subject to higher error, so these data are best removed. Line segments in which direction changes occurred were removed using INTREPID's `splitcruise` tool. This tool is also used to split survey lines into relatively straight line segments. This is because levelling requires lines with constant bearing and splitting ship-tracks into straight-line segments then avoids multiple cross-overs for the same pair of lines and allows rapid location of cross-overs.

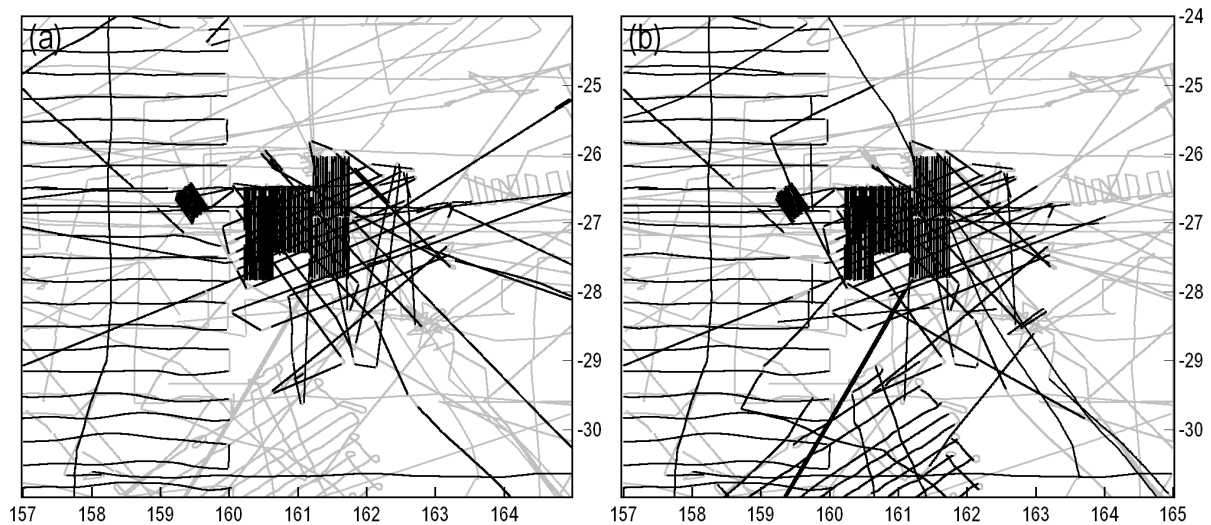


Figure 5.1: Map showing ship-tracks in the Capel/Faust area before and after line splitting and editing. The original ship tracks, not all with gravity and/or magnetic data, are shown by the grey lines. The black lines show the tracks used for levelling (a) gravity data and (b) magnetic data (i.e. after splitting the tracks into straight-line segments and after editing to remove close or problematic tracks).

The `splitcruise` tool requires parameters to be set that define when a line is to be split. These include an angle defining the maximum allowable direction change, an angle and a distance (number of samples) over which gradual changes in line direction are detected, the minimum number of points required for a line segment (avoids preserving extremely short line segments) and a maximum allowable distance between samples (to break a line where data are missing). After experimenting with various parameters, those shown in Table 3 were adopted. These parameters are different to those used previously by INTREPID GEOPHYSICS (DFA, 2001), but experimentation showed that these parameters provided a suitable dataset with appropriate line breaks (Figure 5.1).

Table 3: Parameters used for the Intrepid™ splitcruise process. Different data sampling rates required different values for the previously-levelled dataset and the GA-302/GA-2436 datasets. The maximum-distance parameter is in the same units as the coordinate system of the dataset (degrees in this case, so lines are effectively not split at any gap length).

| PARAMETER | PREVIOUSLY LEVELLED | GA-302 GA-2436 |
|-------------------------------|------------------------|-------------------|
| SharpAngleTolerance | 20 | 20 |
| TrendAngleTolerance | 20 | 20 |
| TrendDistanceInSamples | 10 | 100 |
| MinimumSamplesBeforeDrop | 150 | 800 |
| MaximumDistanceBetweenSamples | 10000 | 10000 |

5.1.3 Line filtering

Gravity and magnetic data from the GA-302 and GA-2436 surveys were line filtered to smooth the data and remove spurious data (Fugro Robertson, 2007; 2008). The previously-levelled dataset appears not to have been filtered and many lines retained significant high-frequency noise. This noise degrades the levelling as it is difficult to determine a truly representative mistie value at line cross-overs. Therefore, these data were also line filtered prior to levelling.

The line filtering was carried out using the `linefilter` tool in the INTREPID™ software. A Fuller low-pass spatial filter was used with a window size of 40 data points for the gravity data and 35 data points for the magnetic data. Figure 5.2 shows examples of line data before and after filtering.

After the previously-levelled dataset was line filtered, the three separate datasets were merged to provide a single database with consistent data fields (Figure 5.1).

5.1.4 Line-levelling method

The Intrepid `marinelevel` tool calculates misclosures at line cross-overs and then performs a network adjustment to minimise the misclosure errors throughout the survey area. Several different methods for the network adjustment are available. These include methods that apply a constant shift to the whole dataset or on a line-by-line basis (`LevelDC`, `LevelLinesDC`) or by adjusting the survey data using piece-wise linear interpretation (`LevelDrape`, `LevelSurface`). These methods all require a reference dataset to which the survey data are tied. The reference dataset might be a recent, high-quality dataset to which other datasets can be tied with confidence. In the case of gravity data, the survey lines can be adjusted against a regional, satellite-derived dataset. This is the approach that was used to level the Australia-wide dataset in 2001 (Section 2.3.1) (DFA, 2001; Petkovic et al., 2001).

Two other levelling methods are available, both of which do not necessarily require a reference dataset. A loop-levelling approach (`LevelLoop`) involves distributing misclosures (misties) around closed loops using standard network adjustment methods. The distributed misclosure errors are then used to define a correction function. A polynomial-based levelling technique (`LevelPolynomial`) computes a correction function based on a piece-wise defined polynomial that is fit to the raw misclosure data after smoothing.

Once the correction function is computed for each survey (or from a combined dataset), adjustments are calculated at every observation point by interpolating a value from the correction function. The interpolation is made using an Akima spline, optionally out to a certain distance, beyond which linear interpolation is used.

Several other parameters and options must be considered and set. These are:

- `ByCruise`: determines whether or not lines without any cross-overs are levelled. If yes, then the levelling corrections are applied to the whole of a cruise/survey (identified by the `FlightNumber` alias in the Intrepid database) on the basis of the correction function for that survey. Note that the correction function is defined for the whole of a cruise area, so an adjustment value can be interpolated from the correction function for all lines, even those without cross-overs.

- `DoPseudoFidsAsRecords`: marine levelling requires a fiducial (FID) field, but if this field doesn't exist then a pseudo FID is computed from cumulative distance. In this case, the different datasets had inconsistent FIDs, so new ones were generated as part of the levelling process.
- `SaveEmptyGroupsInXover`: allows line segments without cross-overs to be included in the cross-over dataset.
- `DuplicateCrossOver_Fid_Tolerance`: if two cross-overs are within a certain distance of each other, one is rejected. This avoids levelling instabilities caused by extreme gradients between points that are too close (even small differences can induce extreme gradients). This tolerance is checked as the levelling adjustments are applied because the cross-over dataset includes all cross-overs, regardless of how close they are. Units are as for coordinates.
- `MaximumPointSeparation`: if adjacent data points around a line cross-over are too widely spaced, then the misclosure value is deemed unreliable and excluded. Units are as for coordinates.
- `MaximumInterpolationGap`: controls the use of spline or linear interpolation when interpolating an adjustment value from the correction function. Units are as for the fiducial field.

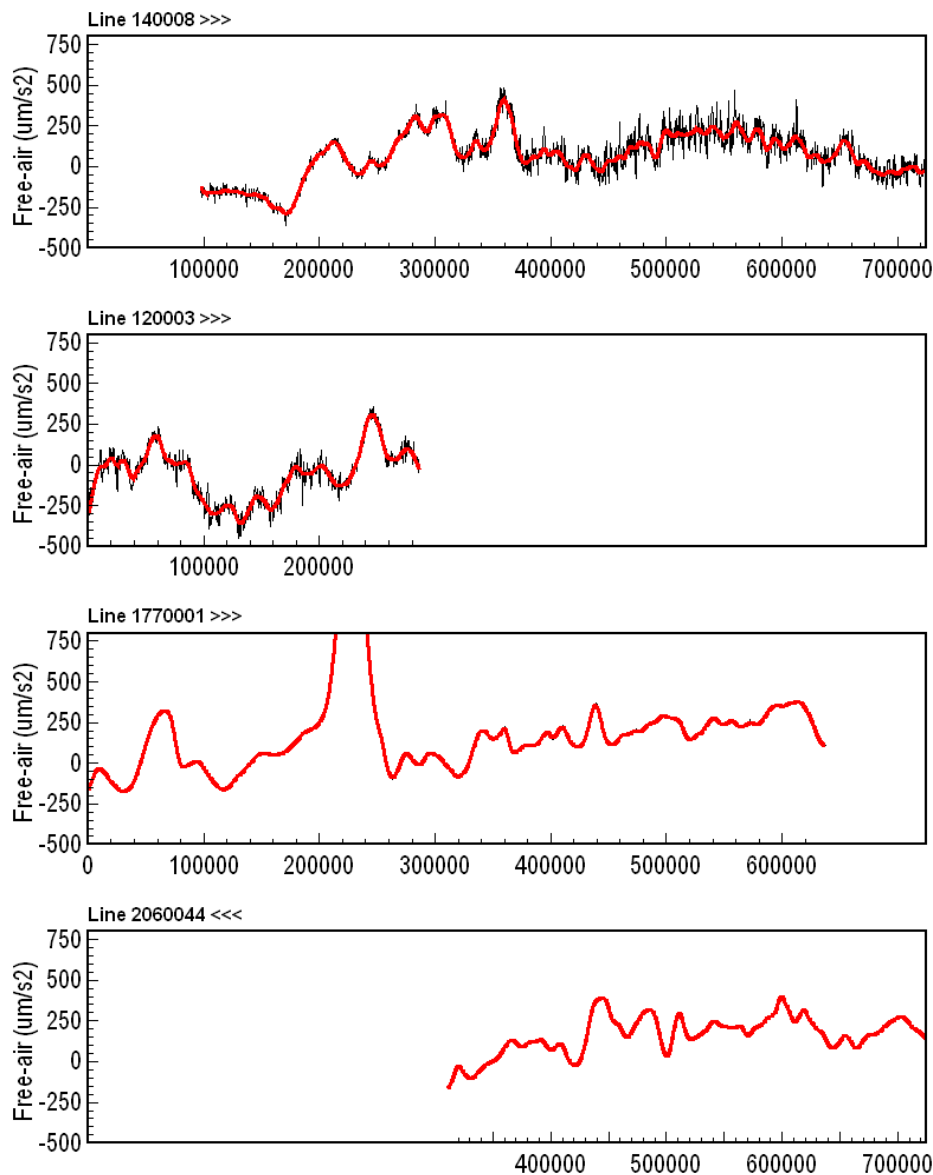


Figure 5.2: Example profiles of ship-track free-air gravity before (black lines) and after application of a Fuller low-pass filter (red lines). Profiles show projected distance (in metres) along each line relative to longitude 157°E. The upper two profiles show noisy data, whereas the lower, more-recently acquired profiles are less noisy. It is unclear whether these profiles were previously filtered.

For polynomial levelling, the following parameters must also be set:

- **Width:** defines the number of cross-over points (window) to use for the piecewise definition of the polynomial correction function.
- **Order:** order of the polynomial fit.
- **MinNpts:** specifies the minimum number of cross-over points in a line before the polynomial will be computed.
- **ConvolveWidth:** specifies the width (in data points) of the convolution filter used to smooth the polynomial fit to cross-overs prior to computation of levelling corrections. Though it is not stated, a value of -1 is assumed to exclude this smoothing process.
- **DistanceWeighted:** biases the polynomial correction function according to the distance from clusters of cross-overs.

The levelling of the Capel/Faust combined dataset used the loop-levelling technique for magnetic data and the polynomial levelling method for gravity data. These methods were used previously to generate the Australia-wide levelled datasets (DFA, 2001; Petkovic et al., 2001). The following sections provide further information on the levelling of the Capel/Faust gravity and magnetic data.

5.2 GRAVITY DATA LEVELLING

5.2.1 Line editing

Initial levelling trials demonstrated that despite the automatic line editing performed during the line splitting process, many problem lines or line segments remained. These line segments were either too short or too close to other, generally more continuous lines and resulted in spurious levelling results. Therefore, additional line editing was carried out using the INTREPID™ Flight Path Editor. Table 4 shows the lines that were either deleted or trimmed.

Table 4: List of surveys and lines that were excluded from gravity levelling due to their short length or proximity to other lines. The label ‘e’ after the line number indicates that the end of a line was deleted and a label ‘t’ indicates that this line was set as a tie-line (to avoid gridding problems).

| SURVEY | YEAR | LINE NUMBERS (AS DEFINED DURING <code>splitcruise</code> PROCESS) |
|---------|------|---|
| GA-12 | 1971 | 27, 34e |
| GA-13 | 1971 | 01t |
| GA-14 | 1971 | 04, 02 |
| GA-1152 | 1994 | 04 |
| GA-1622 | 1977 | 01t |
| GA-206 | 1998 | 09, 12e, 40, 42, 47e, 49 |
| GA-302 | 2006 | 21, 34, 36, 45, 46, 48, 51, 77, 87 |

5.2.2 Levelling

After trialling several different methods and combinations of parameters, the final levelled gravity data were generated using the polynomial levelling method (`LevelPolynomial`) and a reference dataset. The line data were levelled using a reference dataset that combined DNSC08GRA ([Section 2.1.2](#)) and data from the GA-2436 survey. Earlier levelling attempts used only the satellite-based data as a reference. However, this approach tended to smooth out shorter wavelength anomalies evident in the high-resolution GA-2436 data. The reference dataset was prepared by merging a grid of the DNSC08GRA data with a grid of the GA-2436 data, then converting this grid into a line dataset that comprises a series of north–south and east–west lines with a separation equivalent to the cell size of the original merged grid (0.01°).

The parameters used in the `marinelevel` tool for levelling the gravity data are shown in [Table 5](#) and the gridded line-levelled free-air data are shown in [Figure 5.3](#). Mistie statistics at line cross-overs before and after levelling are shown in [Table 6](#).

Table 5: Parameters used for polynomial-based levelling of gravity data.

| PARAMETER | VALUE | COMMENT |
|----------------------------------|-----------------|---|
| RunType | LevelPolynomial | |
| ByCruise | Yes | |
| PopulationAnalysis | No | |
| DoPseudoFidsAsRecords | Yes | |
| SaveEmptyGroupsInXover | Yes | |
| DuplicateCrossOver_Fid_Tolerance | 0.02 | Same units as database coordinates (°, ~2.2 km) |
| MaximumPointSeparation | 10000 | i.e. assume no gap is too large |
| MaximumInterpolationGap | 10000 | i.e. spline interpolation used everywhere |
| Polynomial width | 5 | |
| Polynomial order | 1 | linear |
| Polynomial MinNpts | 2 | |
| Polynomial ConvolveWidth | -1 | no smoothing |
| WeightMethod | Unity | no weighting |

Table 6: Free-air anomaly extremes and mistie statistics before and after levelling (values in $\mu\text{m/s}^2$).

| | MINIMUM | MAXIMUM | MEAN | MEDIAN | SD |
|------------------|---------|---------|------|--------|------|
| Before levelling | -1125 | 2128 | 41.3 | 36.6 | 57.7 |
| After levelling | -364 | 2155 | 3.9 | 7.9 | 20.3 |

5.3 MAGNETIC DATA LEVELLING

5.3.1 Line editing

As for the gravity data, short lines and lines (or line segments) located close to longer lines were deleted to improve the levelling process. Closed loops could not be generated for some isolated lines at the extremities of the dataset and these were also removed. The deleted or edited lines are shown in Table 7.

Table 7: List of surveys and lines that were excluded from magnetic levelling due to their short length or proximity to other lines. The label 'e' after the line number indicates that only the end of a line was deleted and a label 't' indicates that this line was set as a tie-line (to avoid gridding problems).

| SURVEY | YEAR | LINE NUMBERS (AS DEFINED DURING <code>splitcruise</code> PROCESS) |
|---------|------|---|
| GA-12 | 1971 | 16, 23, 26, 27, 34e |
| GA-13 | 1971 | 01t |
| GA-14 | 1971 | 02, 04 |
| GA-15 | 1971 | 01, 03, 07, 08, 12, 20, 22 |
| GA-1151 | 1972 | 04t |
| GA-1152 | 1994 | 04 |
| GA-1377 | 1968 | 02 |
| GA-1504 | 1971 | 11 |
| GA-1592 | 1967 | 01e |
| GA-1622 | 1977 | 01t |
| GA-206 | 1998 | 09, 12e, 39e, 40, 42, 44e, 47e, 49 |
| GA-2436 | 2007 | 02, 03, 04, 05, 126 |
| GA-302 | 2006 | 21, 34, 36, 45, 46, 48, 51, 74, 77, 81, 87, 88e |
| GA-52 | 1985 | 01, 18, 19, 27, 65 |

5.3.2 Levelling

Unlike the gravity data, magnetic data cannot be levelled against a reference dataset. The magnetic data were therefore levelled using the loop levelling method (`LevelLoop`). The parameters used in the `marinelevel` tool for levelling the magnetic data are shown in Table 8 and the gridded magnetic anomaly data are shown in Figure 5.4. Mistie statistics at line cross-overs after levelling (Table 9) indicate a significant improvement compared to the results prior to levelling.

Table 8: *Parameters used to loop-level the magnetic data.*

| PARAMETER | VALUE | COMMENT |
|----------------------------------|-----------|---|
| RunType | LevelLoop | |
| ByCruise | Yes | |
| PopulationAnalysis | No | |
| DoPseudoFidsAsRecords | Yes | |
| SaveEmptyGroupsInXover | Yes | |
| DuplicateCrossOver_Fid_Tolerance | 0.02 | Same units as database coordinates (°, ~2.2 km) |
| MaximumPointSeparation | 10000 | i.e. no gap too big |
| MaximumInterpolationGap | 10000 | i.e. spline interpolation used everywhere |

Table 9: *Magnetic anomaly extremes and mistie statistics before and after levelling (values in nT).*

| | MINIMUM | MAXIMUM | MEAN | MEDIAN | SD |
|------------------|---------|---------|------|--------|------|
| Before levelling | -750 | 1097 | 17.8 | 6.9 | 28.6 |
| After levelling | -586 | 1104 | 0.2 | 0.2 | 1.1 |

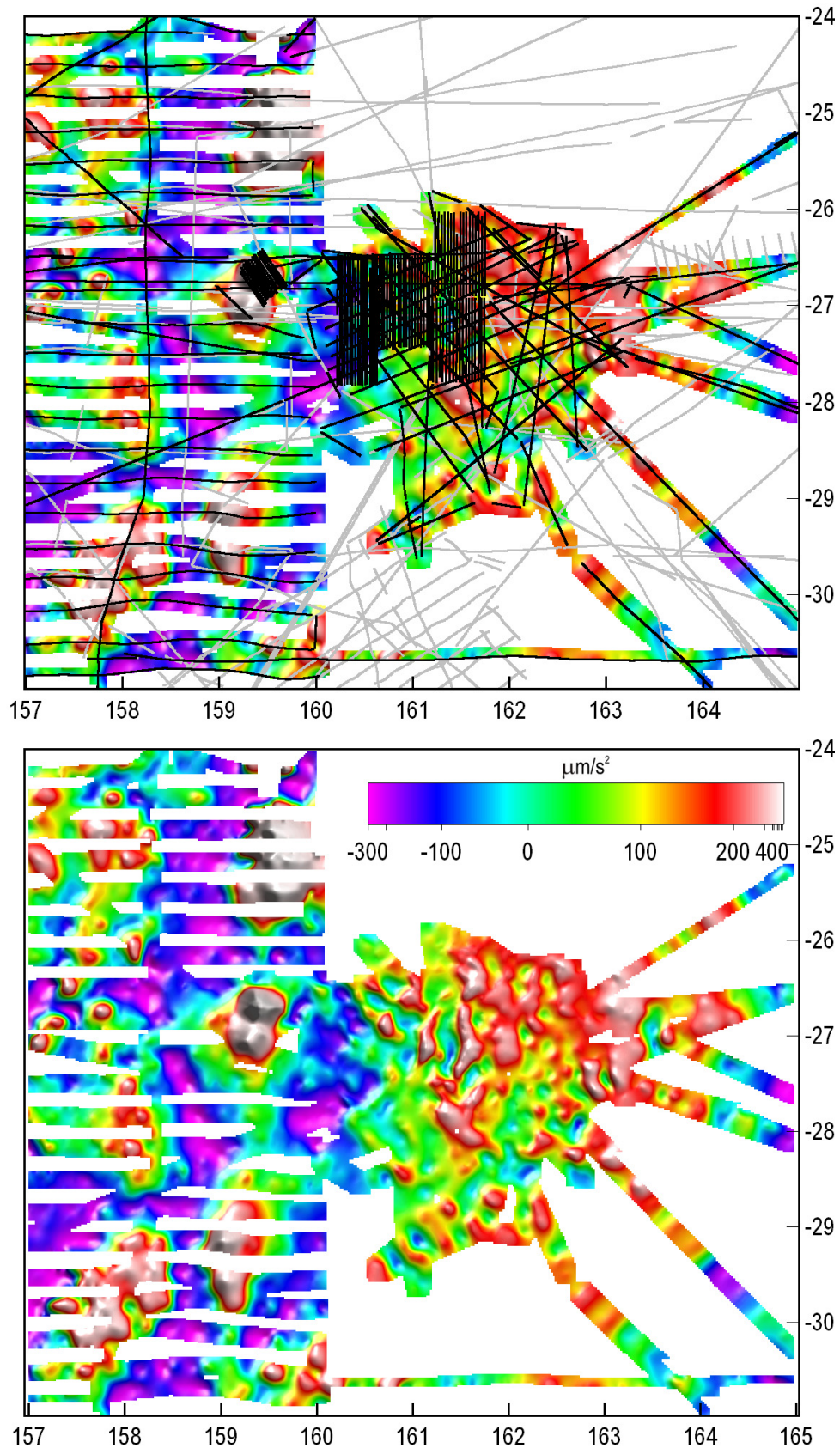


Figure 5.3: Maps showing levelled free-air anomalies ($\mu\text{m/s}^2$). In (a), black lines show the ship-tracks with gravity data that were levelled, whereas the grey lines show all ship-tracks, not all of which have gravity data and some of which were removed from the levelling process due to their proximity to other tracks or due to spurious data.

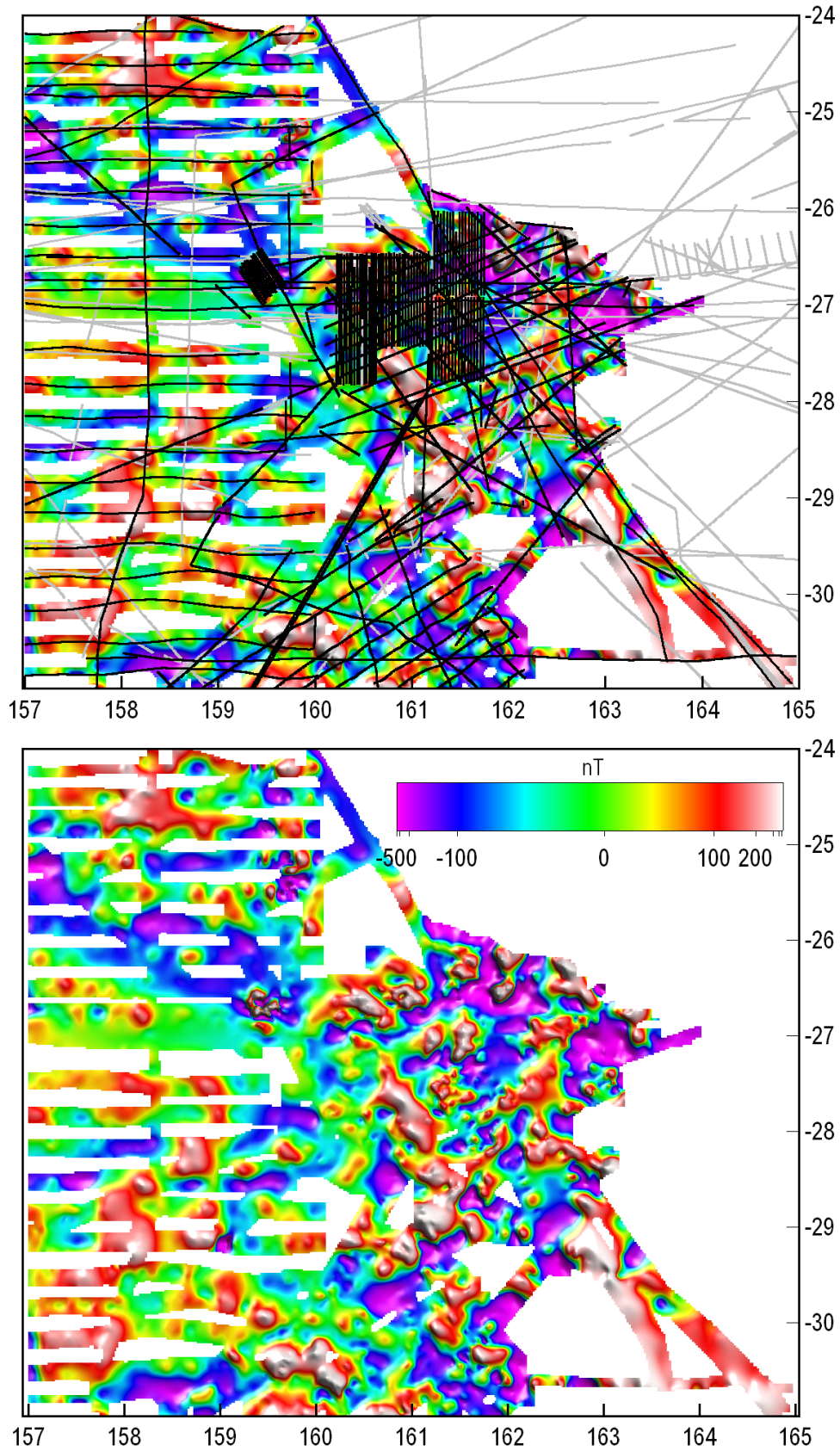


Figure 5.4: Maps showing levelled magnetic anomalies (nT). In (a), black lines show the ship-tracks with magnetic data that were levelled, whereas the grey lines show all ship-tracks, not all of which have magnetic data and some of which were removed from the levelling process due to their proximity to other tracks or due to spurious data.

6 Further data processing

The levelled line data described in [Section 5](#) were gridded in INTREPID™ using a 0.02° grid cell size ([Figure 5.3](#) and [Figure 5.4](#)). Further processing of these grid data has been carried out to aid geological interpretation.

6.1 GRAVITY DATA

6.1.1 Bouguer anomaly

In marine areas, the large density contrast at the seafloor (sea water versus sediment) means that the free-air anomaly retains a strong correlation with bathymetry (compare [Figure 3.1](#) and [Figure 5.3](#)). Free-air anomalies are more positive over the Lord Howe Rise than over the adjacent Middleton Basin to the west. This results in a westward-decreasing gradient in the free-air gravity data. The correlation between free-air gravity and bathymetry can be accounted for by applying the Bouguer correction. This correction removes the gravity effect of the large density contrast at the seafloor by assuming that the seawater is replaced by rock with a density that minimises the correlation with bathymetry.

Bouguer corrections for a spherical cap were computed using the INTREPID™ Gravity Field Reduction tool (Argast et al., 2009). The density contrast between sea water and sediment was set to 970 kg/m³ (i.e. the sediment density was assumed to be 2000 kg/m³, sea water 1030 kg/m³) and the resulting Bouguer anomaly map is shown in [Figure 6.1](#). The lowest Bouguer anomalies exist over the eastern parts of the GA-302 survey area where the water depth is shallowest and the crust is thickest (i.e. Lord Howe Platform, cf. [Figure 1.1](#)). The highest values exist over the Middleton Basin region where water depths are greatest and crustal thickness reduces.

6.1.2 Band-pass filtering

Short-wavelength anomalies are evident in the Bouguer gravity map ([Figure 6.1](#)), but they are obscured in part by the long-wavelength variations induced by changes in crustal thickness. Various methods exist to highlight the short-wavelength gravity features that are important for geological interpretation. These methods include regional-residual field separation techniques, filtering, isostatic modelling and other image enhancement techniques. For the purposes of removing long-wavelength components in the Capel/Faust Bouguer gravity field, a band-pass filter was applied using the INTREPID™ fast-Fourier transform grid filtering tool. The low-pass cut-off was set at a wavelength of 8 km and the high-pass cut-off at 100 km. This filter window served to remove the long-wavelength component of the Bouguer anomaly related to crustal thickness variations and also further smoothed the data ([Figure 6.2](#)).

The band-pass filtered Bouguer data correlate well with basement highs and depocentres evident in the GA-302 seismic reflection data ([Figure 6.3](#)). Given this correlation, the gravity data have proven to be a useful additional constraint during the interpretation of the GA-302 seismic data and for structural mapping of the Capel and Faust basins (cf. Higgins et al., in prep.). This is because the seismic reflection data, the primary dataset for interpretation, is two-dimensional and line separation is ~20 km at best, but up to ~50 km. Gravity data, particularly the data collected on the closely-spaced (~4 km) lines of the GA-2436 survey, provide a means to link structures between seismic lines. The data have also been used to analyse the dominant structural trends associated with the formation of the Capel and Faust basins (Higgins et al., in prep.) and, after application of additional corrections, to constrain 3D potential field modelling to test interpretations of depth-to-basement and basin architecture (Petkovic et al., 2010; in prep.).

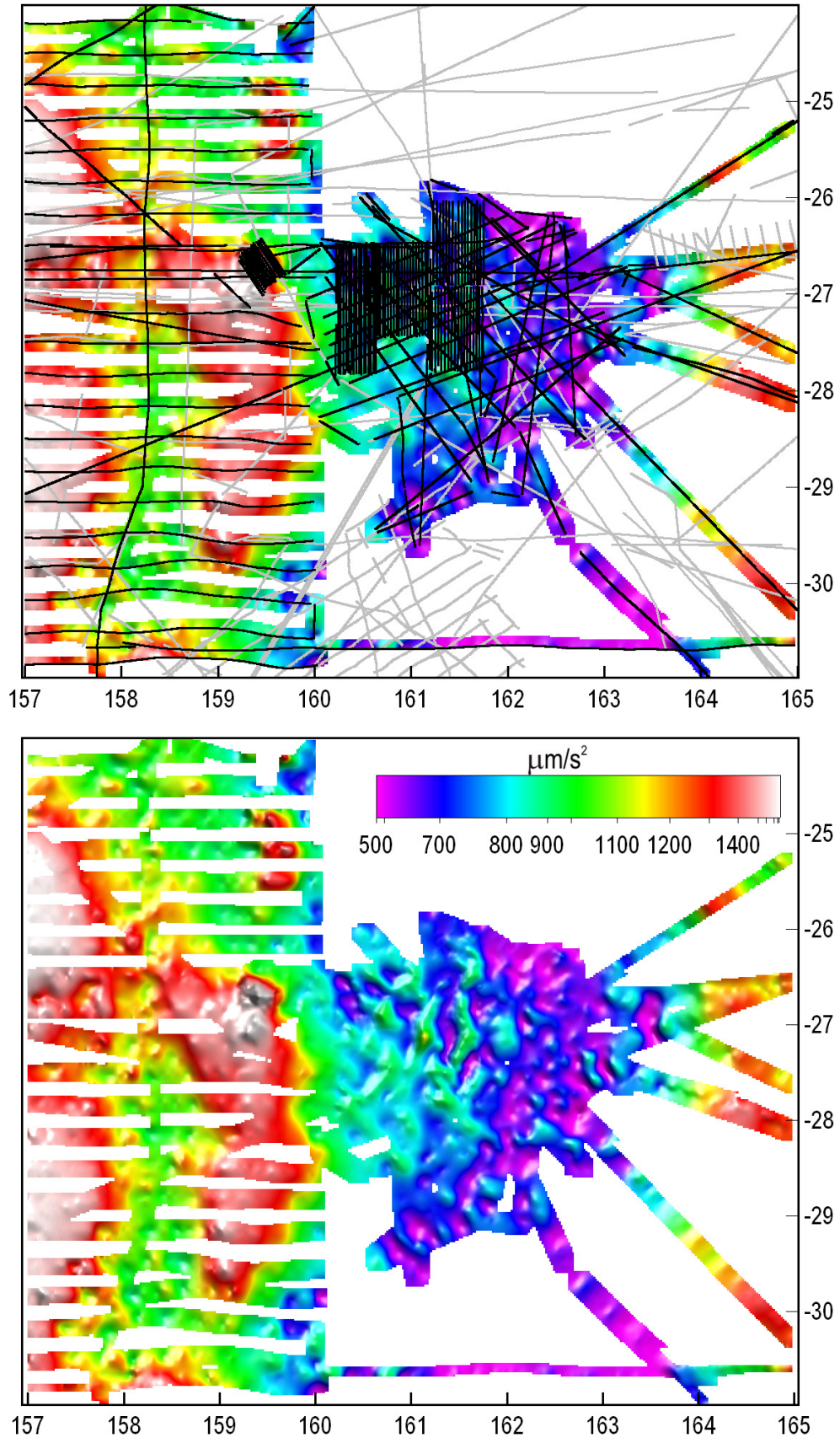


Figure 6.1: Simple Bouguer anomalies ($\mu\text{m/s}^2$) computed from the levelled free-air gravity data using a spherical cap Bouguer correction and a sea-water/sediment density contrast of 970 kg/m^3 . Black and grey lines are as in Figure 5.3.

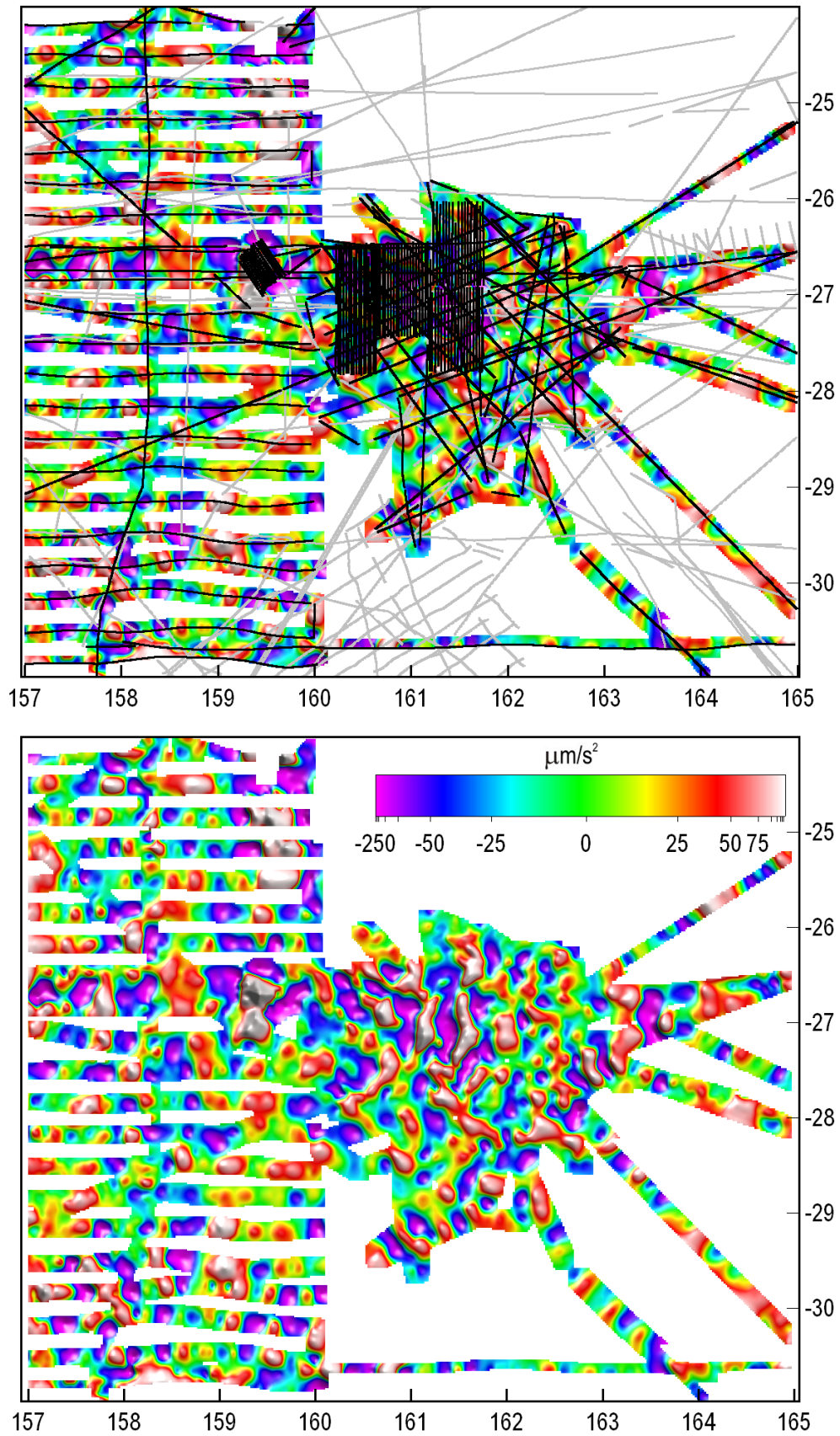


Figure 6.2: Band-pass filtered Bouguer gravity data ($\mu\text{m/s}^2$) preserving wavelengths between 8 and 100 km. Black and grey lines are as in Figure 5.3.

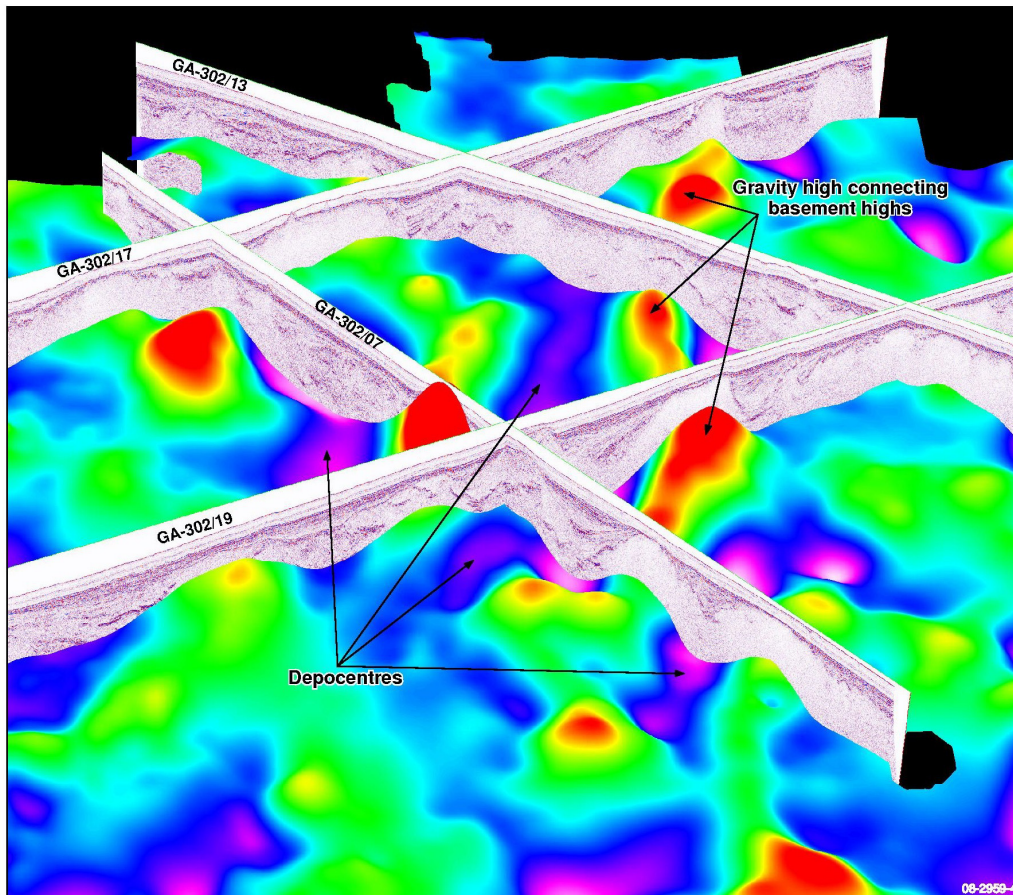


Figure 6.3: Perspective view looking to the NNE across the northwestern part of the GA-302 survey area showing selected seismic lines and band-pass filtered Bouguer gravity anomalies (arbitrarily shifted and scaled to plot with the seismic data).

6.2 MAGNETIC DATA

6.2.1 Reduction to pole

While gravity anomalies tend to lie directly over their source, the same is only true for magnetic anomalies when the rock magnetisation direction and the external magnetic field are vertical (i.e. at the magnetic poles). Away from the magnetic poles, magnetic anomalies tend to be characterised by a positive–negative couple that makes the anomalies more complicated to interpret. This complication can be accounted for by reducing all the anomalies to the pole, i.e. modifying the anomaly to the form it would have for vertical magnetisation and external field orientation (Blakely, 1996).

Reduced-to-pole magnetic anomalies based on the levelled dataset are shown in [Figure 6.4a](#). The pole reduction was computed for the central latitude of the Capel/Faust region (161°E/-27.5°S) for field parameters on 1 January 2007 (field inclination -56.12°, declination 13.0°). However, given that the new levelled dataset comprises data spanning several decades, the use of a single date for the reduction-to-pole possibly induces some errors. The oldest data retained in the levelled dataset are from 1967 (survey GA-1592) and if the data are reduced-to-pole using IGRF parameters from 1 January 1967 (field inclination -56.04°, declination 12.3°; [Figure 6.4b](#)), the difference is insignificant ([Figure 6.4c](#)).

The reduced-to-pole magnetic anomaly grid was further smoothed by applying a low-pass filter with a cut-off wavelength at 15 km ([Figure 6.5](#)).

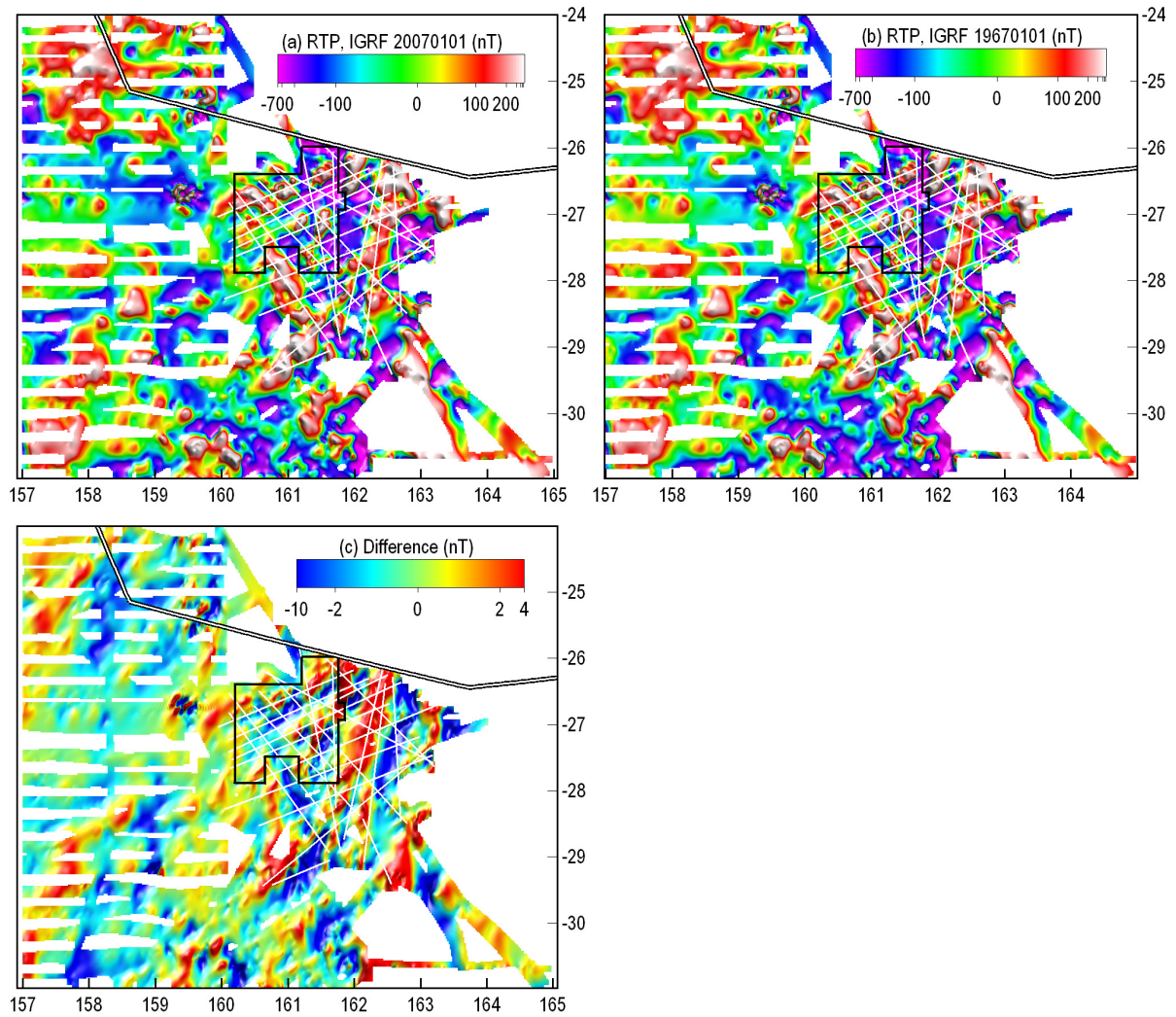


Figure 6.4: Reduced-to-pole magnetic anomalies (in nT) computed using IGRF parameters for (a) 1 January 2007 and (b) 1 January, 1967. (c) The difference between these two grids. The GA-302 seismic lines are shown in white and the GA-2436 survey area is outlined by the black polygon. The white-on-black line is the limit of Australia's marine jurisdiction (see Figure 1.1 for details). Note that though they are not evident in these images, ringing artefacts are present in the vicinity of the Gifford Guyot (centred on 159.5°E/26.7°S), a steep-flanked, basaltic seamount that rises from about 2500 m water depth to within about 300 m of the sea surface (Heap et al., 2009). These artefacts result from the application of fast-Fourier transform methods to compute the pole reduction.

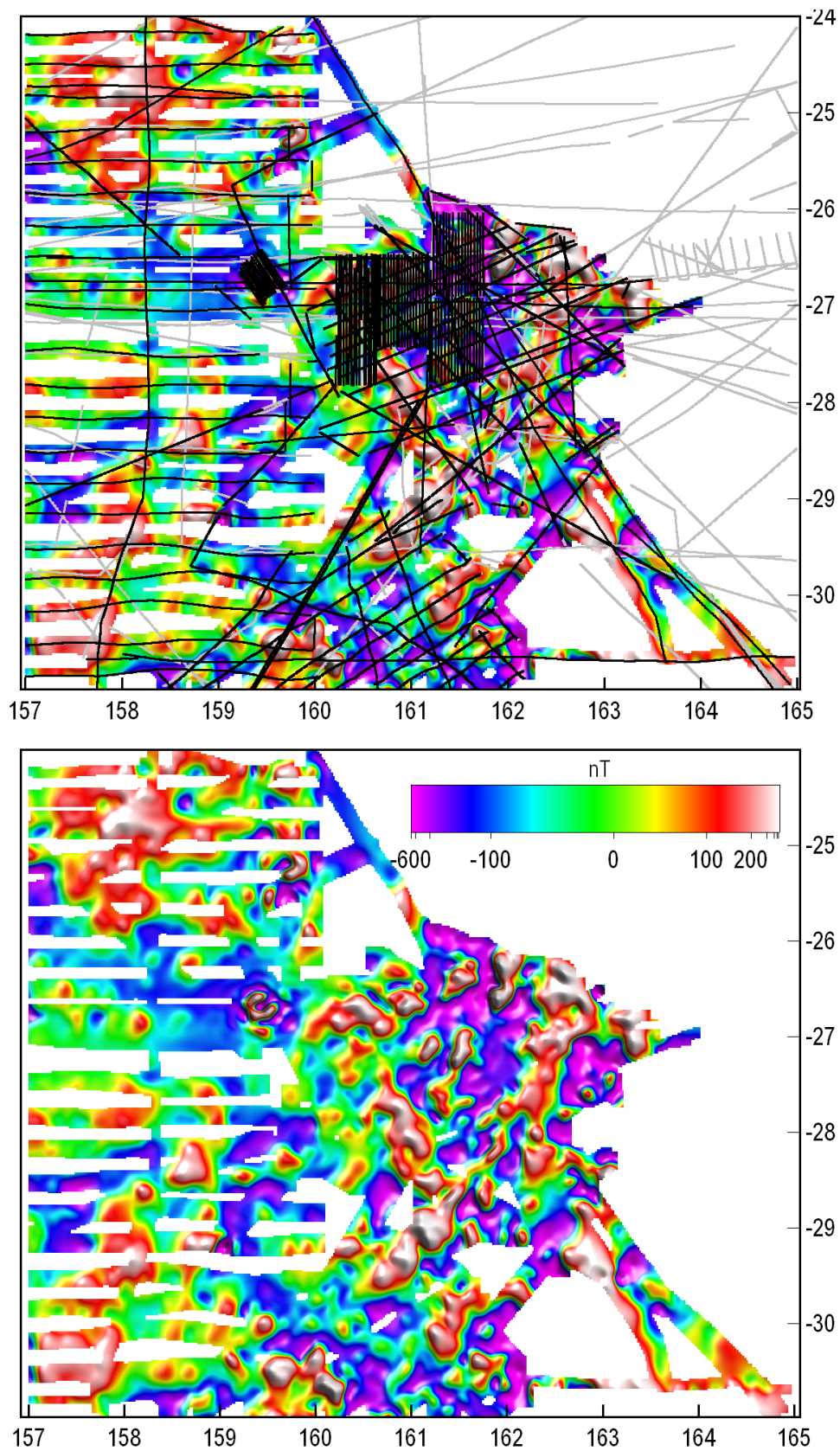


Figure 6.5: Low-pass filtered (cut-off wavelength 15 km), reduced-to-pole magnetic anomalies (nT). Black and grey lines in (a) are as in Figure 5.4. Note that ringing artefacts are evident in the vicinity of the Gifford Guyot (centred on 159.5°E/26.7°S), a steep-flanked, basaltic seamount that rises from about 2500 m water depth to within about 300 m of the sea surface (Heap et al., 2009).

7 Summary

The potential field dataset described in this record represents a key output from Geoscience Australia's Remote Eastern Frontiers Project. The dataset complements other datasets, primarily seismic reflection data from Survey GA-302, and is a key constraint on interpretation of the structures that have influenced basin formation and the depth of sediment depocentres. The data also complement and improve on regional compilations of marine and satellite-derived data in this region.

The levelled dataset and gridded versions of the levelled gravity and magnetic data are available on the CD accompanying this record ([Section 8](#)). Regional datasets covering the Tasman Sea region, including magnetic data from a global compilation and satellite-altimetry derived gravity data, are also provided as they allow interpretations in the Capel and Faust basins to be extended and placed into a regional tectonic context. These regional datasets are also useful for future planning of surveys aimed at exploring other frontier basins on the Lord Howe Rise and on other parts of the Australian margin.

Acknowledgements

I thank Des Fitzgerald and Ray Seikel for advice on using the INTREPID GEOPHYSICS levelling tools, Peter Petkovic, Michael Morse and Mike Sexton for help with locating and dealing with data, and Michael Morse, Ray Tracey and Nadege Rollet for comments on earlier versions of this record. This Record is published with the permission of the Chief Executive Officer, Geoscience Australia.

8 Appendix: data description

This Appendix describes the data provided with this record on the accompanying CD-ROM. The line data are also available from the Geophysical Archive Data Delivery System (www.ga.gov.au/gadds).

8.1 FILE-NAMING CONVENTION

Filename format is of the form:

```
ddd_REG_[description]_PROJ_YYYYMMDD.xxx
```

where

- ddd: data type, mag denotes magnetic data and grv denotes gravity data;
- REG: region code chosen to be consistent with Geoscience Australia provinces database. Most files provided here include CAP as the region code (for Capel Basin, in this case also referring to Faust Basin), but externally-sourced regional datasets (Section 8.3.2) include the non-standard region code EAU (for Eastern Australia);
- [description]: free-text field indicative of data content;
- PROJ: projection, GEOD is geodetic coordinates; UTM57S = UTM Zone 57S. Files provided here all use the WGS84 datum;
- YYYYMMDD: year, month and day on which file was first generated (equivalent to a “version number”);
- xxx = file extension (e.g. .ers is ER Mapper grid, .asc = column-based ascii file).

8.2 DATA FILES

8.2.1 Data for surveys GA-302 and GA-2436

Directory on CD: `data/capel-faust/line/fugro`

Table 10 lists the Fugro Robertson processing reports and data files containing gravity and magnetic data for the GA-302 and GA-2436 surveys.

Table 10: *Data files and processing reports from Fugro Robertson for surveys GA-302 and GA-2436.*

| FILENAME | DESCRIPTION |
|---|---|
| linedata_4640_GA302.asc | Column-based ascii file with gravity and magnetic data from survey GA-302 (as provided by Fugro Robertson) |
| 302_data_proc_4640_Fnl_Rpt.pdf | Processing report for GA-302 gravity and magnetic data |
| linedata_4731_GA_Capel-Faust-Basins.asc | Column-based ascii file with gravity and magnetic data from survey GA-2436 (as provided by Fugro Robertson) |
| Fnl_Rpt_4731_GA_Capel-Faust-Basins.pdf | Processing report for GA-2436 gravity and magnetic data |

8.2.2 Levelled gravity and magnetic data

Directory on CD: `data/capel-faust/line`

The levelled gravity and magnetic data, together with the original data, are provided in two file formats:

- CAP_GravMag_Record2010-34_20100714..DIR: INTREPID™ database
- CAP_GravMag_Record2010-34_20100714.dat: ascii file exported from the INTREPID™ database using the data-definition file CAP_GravMag_Record2010-34_20100714.ddf.

The fields present in these data files are described in Table 11.

Table 11: Description of data fields contained in levelled data files. Longitude and latitude fields are tied to the WGS84 ellipsoid, gravity quantities are in $\mu\text{m/s}^2$, and magnetic quantities are in nT. Note that the INTREPID™ X and Y aliases can be assigned to the different coordinate sets depending on whether levelled and edited gravity or magnetic data are to be dealt with. Null fields are assigned a value of -999999.

| FIELD NAME | INTREPID ALIAS | DESCRIPTION |
|----------------|----------------|---|
| SURVEY | FlightNumber | Geoscience Australia survey number |
| SPLITLINE | LineNumber | Line number resulting from the INTREPID™ splitline process (10 000 x SURVEY + sequential number). Note that these line numbers do not coincide with line numbers associated with Geoscience Australia seismic lines |
| LineType | LineType | Set to 2 for normal survey line and, for a few lines, to 4 for tie lines (to avoid gridding problems) |
| PFID | Fiducial | Pseudo-fiducial field generated by INTREPID™ |
| LONGITUDE | X | WGS84 geodetic longitude |
| LATITUDE | Y | WGS84 geodetic latitude |
| LongGrav | X | Coordinate set in which deleted gravity line segments are nulled (Section 5.2.1) |
| LatGrav | Y | |
| LongMag | X | Coordinate set in which deleted magnetic line segments are nulled (Section 5.3.1) |
| LatMag | Y | |
| AUSBATH09 | | Water depth interpolated from the Australian Bathymetry and Topography Grid (Whiteway, 2009) |
| ObsGravRev | | Observed gravity reverse-computed from FreeAir4Lev (Section 5.1.1) |
| FreeAir4Lev | | Free-air gravity data to be levelled |
| FreeAirLevPoly | | Free-air anomaly values after polynomial levelling (Section 5.2.2) |
| simpleBouguer | | Simple Bouguer anomaly computed using a spherical cap and a correction density of 970 kg/m^3 (Section 6.1.1). |
| MagAnom4Lev | | Magnetic anomaly data to be levelled |
| MagAnomLevLoop | | Magnetic anomaly values after loop levelling (Section 5.3.2) |

8.2.3 Shape files

Directory on CD: data/capel-faust/line

ESRI shape files containing survey lines (ship tracks) are also provided (Table 12).

Table 12: List of shape files containing all ship tracks and tracks containing only levelled gravity and magnetic data (cf. Figure 5.1). Associated .dbf and .shx files are included for each.

| FILENAME | DESCRIPTION |
|--|--|
| CAP_all_lines_GEOD_20100330.shp | All ship-tracks (lines) in the Capel/Faust region that were collated for this work |
| grv_CAP_levelled_lines_GEOD_20100330.shp | Only lines with levelled gravity data |
| mag_CAP_levelled_lines_GEOD_20100330.shp | Only lines with levelled magnetic data |

8.3 GRIDDED DATA

8.3.1 Grids of levelled data

Directory on CD: data/capel-faust/grid

For convenience, gridded versions of the levelled datasets are also provided on the CD accompanying this record. These grids are provided in ER Mapper format (.ers) and as geo-located TIFF files (.tif). Table 13 lists the data grids that are provided.

Table 13: List of grid files derived from levelled data. Cell size for each grid is 0.02° and the extrapolation limit is five grid cells (i.e. the distance from data points beyond which grid interpolation is truncated). Gravity units are $\mu\text{m/s}^2$ and magnetic units are nT.

| GRID NAME | DESCRIPTION |
|---|--|
| grv_CAP_LevFreeAir_GEOD_20100304.xxx | Grid of levelled free-air gravity data |
| grv_CAP_LevBA2000_GEOD_20100304.xxx | Grid of simple Bouguer anomaly computed using a spherical cap and with a correction density of 970 kg/m ³ (contrast between water and rock) |
| grv_CAP_LevBA2000_BP8-100_GEOD_20100304.xxx | As above, band-pass filtered to preserve wavelengths in the range 8–100 km |
| mag_CAP_Lev_GEOD_20100301.xxx | Grid of levelled magnetic anomaly data |
| mag_CAP_LevRTP2007_GEOD_20100301.xxx | Grid of reduced-to-pole magnetic anomaly data (using IGRF parameters from 1 January 2007). Note that ringing artefacts may be evident in the vicinity of the Gifford Guyot (centred on 159.5°E/26.7°S) |
| mag_CAP_LevRTP2007_LP15_GEOD_20100301.xxx | Low-pass filtered, reduced-to-pole magnetic anomaly grid, preserving wavelengths >15 km. Note that ringing artefacts are evident in the vicinity of the Gifford Guyot (centred on 159.5°E/26.7°S) |

8.3.2 Grids of externally-sourced regional data

Directory on CD: data/regional

Regional gravity and magnetic grids of the Tasman Sea region included on the CD are listed in Table 14. These grids are also provided in ER Mapper format (.ers) and as geo-located TIFF files (.tif).

Table 14: List of regional gravity and magnetic grid files. The cell-size for gravity grids is 1 arc minute and for magnetic grids is 2 arc minutes. Gravity units are $\mu\text{m/s}^2$ and magnetic units are nT.

| GRID NAME | DESCRIPTION |
|---|--|
| grv_EAU_DNSC08GRA_GEOD_20090113.xxx | Free-air gravity based on satellite altimetry from the Danish National Space Centre (Andersen et al., 2010a) |
| grv_EAU_DNSC08_BA2000_GEOD_20100504.xxx | Simple Bouguer anomaly grid derived from the DNSC08GRA free-air data using water depths from the Australian Bathymetry and Topography Grid (Whiteway, 2009) and an infinite-slab correction with a correction density of 970 kg/m ³ (contrast between water and rock) |
| grv_EAU_BA2000-UC25_GEOD_20100504.xxx | Residual Bouguer grid derived by subtracting upward-continued (by 25 km) Bouguer gravity |
| mag_EAU_EMAG2_GEOD_20100329.xxx | Grid of globally-compiled magnetic anomaly data from the EMAG2 dataset (Maus et al., 2009) with a grid-cell size of 2 arc minutes |

References

- Andersen, O.B. and Knudsen, P., 2000. The role of satellite altimetry in gravity field modelling in coastal areas. *Physics and Chemistry of the Earth*, **25**(1), 17-24
- Andersen, O.B., Knudsen, P. and Berry, P., 2010a. The DNSC08GRA global marine gravity field from double retracked satellite altimetry. *Journal of Geodesy*, **84**(3), 191-199, doi:10.1007/s00190-009-0355-9.
- Andersen, O.B., Knudsen, P., Berry, P.A.M., Kenyon, S. and Trimmer, R., 2010b. Recent developments in high-resolution global altimetric gravity field modeling. *The Leading Edge*, **29**, 540-545, doi:10.1190/1.3422451.
- Argast, D., Bacchin, M. and Tracey, R., 2009. An extension of the closed-form solution for the gravity curvature (Bullard B) correction in the marine and airborne cases. *ASEG Extended Abstracts*, **2009**(1), 6pp, doi:10.1071/ASEG2009ab129.
- Blakely, R.J., 1996. Potential theory in gravity and magnetic applications. Cambridge Univ Press, 441 pp.
- Colwell, J.B., Hashimoto, T., Rollet, N., Higgins, K., Bernardel, G. and McGiveron, S., in press. Interpretation of Seismic Data, Capel and Faust Basins, Australia's Remote Offshore Eastern Frontier. Geoscience Australia Record 2010/06
- Deng, X. and Featherstone, W.E., 2006. A coastal retracking system for satellite radar altimeter waveforms: Application to ERS-2 around Australia. *Journal of Geophysical Research*, **111**, C06012, doi:10.1029/2005JC003039.
- DFA, 2001. Reprocessing of south and southeast Australia marine gravity and magnetic data. Intrepid Geophysics, 32pp.
- Fairhead, J.D., Green, C.M. and Odegard, M.E., 2001. Satellite-derived gravity having an impact on marine exploration. *The Leading Edge*, **20**(8), 873-876, doi:10.1190/1.1487298.
- Featherstone, W.E., 2009. Only use ship-track gravity data with caution: a case-study around Australia. *Australian Journal of Earth Sciences*, **56**(2), 195-199, doi:10.1080/08120090802547025.
- Fugro-Robertson, 2007. Shipborne gravity, magnetic and bathymetric survey data processing report, GA302 - Capel and Faust Basins offshore Australia. Fugro Robertson Inc. Job Number 4640, 85pp.
- Fugro-Robertson, 2008. Shipborne gravity, magnetic and bathymetric survey data processing report, Capel and Faust basins: Tangaroa TAN0713. Fugro Robertson Inc. (LCT Gravity & Magnetism Division) Job Number 4731, 90pp.
- Fugro-Seismic, 2007. Seismic data processing report: Capel and Faust basins 2D pre-stack. Fugro Seismic Imaging Pty Ltd, 45pp.
- Gaina, C., Müller, D.R., Royer, J.Y., Stock, J., Hardebeck, J. and Symonds, P., 1998. The tectonic history of the Tasman Sea: a puzzle with 13 pieces. *Journal of Geophysical Research*, **103**(B6), 12413-12433, doi:10.1029/98JB00386.
- Hackney, R.I., Petkovic, P., Hashimoto, T., Higgins, K., Logan, G.A., Bernardel, G., Colwell, J.B., Rollet, N. and Morse, M., 2009. Geophysical studies of Australia's remote eastern deep-water frontier: results from the Capel and Faust basins. *ASEG Extended Abstracts*, **2009**(1), 8pp, doi:10.1071/ASEG2009ab012.
- Hackney, R.J. and Featherstone, W.E., 2003. Geodetic versus geophysical perspectives of the 'gravity anomaly'. *Geophysical Journal International*, **154**(1), 35-43, doi:10.1046/j.1365-246X.2003.01941.x.
- Hashimoto, T., Rollet, N., Higgins, K., Bernardel, G. and Hackney, R., 2008. Capel and Faust basins: Preliminary assessment of an offshore deepwater frontier region. In: J.E. Blevin, B.E. Bradshaw and C. Uruski (Editors), Eastern Australasian Basins Symposium III: Energy security for the 21st century. Petroleum Exploration Society of Australia, Sydney, pp. 311-316.
- Hashimoto, T., Rollet, N., Higgins, K., Petkovic, P., Hackney, R.I. and Fraser, G., 2010. Integrated assessment of the Capel and Faust basins, offshore eastern Australia. *AusGeo News*, **99**, 6pp
- Heap, A., Hashimoto, T. and Rollet, N., 2008. Survey of remote eastern frontier basins completed. *AusGeo News*, **89**, 5pp
- Heap, A.D., Hughes, M., Anderson, T., Nichol, S., Hashimoto, T., Daniell, J., Przeslawski, R., Payne, D., Radke, L. and Shipboard-Party, 2009. Seabed environments and subsurface geology of the Capel & Faust Basins and Gifford Guyot, Eastern Australia - Geoscience Australia TAN0713 post-survey report Geoscience Australia Record 2009/22, 182pp.
- Higgins, K., Hashimoto, T., Hackney, R.I., Petkovic, P. and Milligan, P., in prep. 3D Geological Modelling and Petroleum Prospectivity Assessment in Offshore Frontier Basins using GOCAD™: Capel and Faust Basins, Lord Howe Rise. Geoscience Australia Record

- Hinze, W.J., Aiken, C., Brozena, J., Coakley, B., Dater, D., Flanagan, G., Forsberg, R., Hildenbrand, T., Keller, G.R. and Kellogg, J., 2005. New standards for reducing gravity data: The North American gravity database. *Geophysics*, **70**, J25, doi:10.1190/1.1988183.
- Hwang, C., Guo, J., Deng, X., Hsu, H.Y. and Liu, Y., 2006. Coastal gravity anomalies from retracked Geosat/GM altimetry: improvement, limitation and the role of airborne gravity data. *Journal of Geodesy*, **80**(4), 204-216, doi:10.1007/s00190-006-0052-x.
- Korhonen, J.V., Fairhead, J.D., Hamoudi, M., Hemant, K., Lesur, V., Manda, M., Maus, S., Purucker, M., Ravat, D. and Sazonova, T., 2007. Magnetic Anomaly Map of the World. *Map published by Commission for Geological Map of the World, supported by UNESCO, GTK, Helsinki*
- Kroh, F., Morse, M.P. and Hashimoto, T., 2007. New data on Capel and Faust Basins. *Preview*, **130**(October), 22-24
- Louis, G., Lequentrec-Lalancette, M.F., Royer, J.Y., Rouxel, D., Géli, L., Maïa, M. and Faillot, M., 2010. Ocean Gravity Models From Future Satellite Missions. *EOS, Transactions, American Geophysical Union*, **91**(3), 21-22, doi:10.1029/2010EO030001.
- Maus, S., Sazonova, T., Hemant, K., Fairhead, J.D. and Ravat, D., 2007. National geophysical data center candidate for the world digital magnetic anomaly map. *Geochemistry Geophysics Geosystems*, **8**, Q06017, doi:10.1029/2007GC001643.
- Maus, S., Yin, F., Lühr, H., Manoj, C., Rother, M., Rauberg, J., Michaelis, I., Stolle, C. and Müller, R.D., 2008. Resolution of direction of oceanic magnetic lineations by the sixth-generation lithospheric magnetic field model from CHAMP satellite magnetic measurements. *Geochem. Geophys. Geosyst*, **9**, Q07021, doi:10.1029/2008GC001949.
- Maus, S., Barckhausen, U., Berkenbosch, H., Bournas, N., Brozena, J., Childers, V., Dostaler, F., Fairhead, J.D., Finn, C. and von Frese, R.R.B., 2009. EMAG2: A 2-arc min resolution Earth Magnetic Anomaly Grid compiled from satellite, airborne, and marine magnetic measurements. *Geochemistry Geophysics Geosystems*, **10**(8), Q08005, doi:10.1029/2009GC002471.
- Morse, M., 2010. Potential field methods prove effective for continental margin studies. *AusGeo News*, **98**, 4pp
- Norvick, M.S., Smith, M.A. and Power, M.R., 2001. The plate tectonic evolution of eastern Australasia guided by the stratigraphy of the Gippsland Basin. In: K.C. Hill and T. Bernecker (Editors), Eastern Australasian Basin Symposium, A Refocused Energy Perspective for the Future. Petroleum Exploration Society of Australia, Special Publication, Melbourne, pp. 15-23.
- Norvick, M.S., Langford, R.P., Hashimoto, T., Rollet, N., Higgins, K.L. and Morse, M.P., 2008. New insights into the evolution of the Lord Howe Rise (Capel and Faust basins), offshore eastern Australia, from terrane and geophysical data analysis. In: J.E. Blevin, B.E. Bradshaw and C. Uruski (Editors), Eastern Australasian Basins Symposium III: Energy security for the 21st century. Petroleum Exploration Society of Australia, Sydney, pp. 291-309.
- Petkovic, P., Fitzgerald, D., Brett, J., Morse, M. and Buchanan, C., 2001. Potential Field and Bathymetry Grids of Australia's Margins. *ASEG Extended Abstracts*, **2001**(1), 4pp, doi:10.1071/ASEG2001ab109.
- Petkovic, P., Lane, R., Rollet, N. and Nayak, G.K., 2010. 3D mapping and gravity modelling of Capel and Faust basins. *ASEG Extended Abstracts*, **2010**((1)), 4pp
- Petkovic, P., Lane, R., Rollet, N. and Nayak, G.K., in prep. 3D gravity models of the Capel and Faust Basins, Lord Howe Rise. *Geoscience Australia Record*
- Sandwell, D.T. and Smith, W.H.F., 1997. Marine gravity anomaly from Geosat and ERS 1 satellite altimetry. *Journal of Geophysical Research*, **102**(B5), 10039-10054, doi:10.1029/96JB03223.
- Sandwell, D.T., Smith, W.H.F., Gille, S., Jayne, S., Soofi, K. and Coakley, B., 2001. Bathymetry from Space: White paper in support of a high-resolution, ocean altimeter mission. http://topex.ucsd.edu/marine_grav/white_paper.pdf.
- Sandwell, D.T. and Smith, W.H.F., 2009. Global marine gravity from retracked Geosat and ERS-1 altimetry: Ridge segmentation versus spreading rate. *Journal of Geophysical Research*, **114**, B01411, doi:10.1029/2008JB006008.
- Smith, W.H.F. and Sandwell, D.T., 1997. Global sea floor topography from satellite altimetry and ship depth soundings. *Science*, **277**(5334), 1956-1962, doi:10.1126/science.277.5334.1956.
- Stagg, H.M.J., Borissova, I., Alcock, M.B. and Moore, A.M.G., 1999. Tectonic provinces of the Lord Howe Rise. *AGSO Research Newsletter*, **31**(November), 2pp
- Stagg, H.M.J., Alcock, M.B., Borissova, I. and Moore, A.M.G., 2002. Geological framework of the southern Lord Howe Rise and adjacent areas. *Geoscience Australia Record* 2002/25, 152pp.
- van de Beuque, S., Stagg, H.M.J., Sayers, J., Willcox, J.B. and Symonds, P.A., 2003. Geological framework of the Northern Lord Howe Rise and adjacent areas. *Geoscience Australia Record* 2003/01, 117pp.

- Webster, M. and Petkovic, P., 2005. Australian bathymetry and topography grid: June 2005. Geoscience Australia Record 2005/12, 30pp.
- Whiteway, T.G., 2009. Australian Bathymetry and Topography Grid, June 2009. Geoscience Australia Record 2009/21, 46pp.
- Willcox, J.B., Sayers, J., Stagg, H.M.J. and van de Beuque, S., 2001. Geological framework of the Lord Howe Rise and adjacent ocean basins. In: K.C. Hill and T. Bernecker (Editors), Eastern Australasian Basin Symposium, A Refocused Energy Perspective for the Future. Petroleum Exploration Society of Australia, Special Publication, Melbourne, pp. 211-225.
- Willcox, J.B. and Sayers, J., 2002. Geological framework of the central Lord Howe Rise (Gower Basin) region. Geoscience Australia Record 2002/11, 85pp.